

International Atomic Energy Agency

INDC(SAF)-6/G

INDC

INTERNATIONAL NUCLEAR DATA COMMITTEE

NDS LIBRARY COPY

Progress Report to the INDC
from the Republic of South Africa

1979

Compiled by D. Reitmann

NDS LIBRARY COPY

May 1980

IAEA NUCLEAR DATA SECTION, WAGRAMERSTRASSE 5, A-1400 VIENNA

Reproduced by the IAEA in Austria
May 1980
80-2413

Progress Report to the INDC
from the Republic of South Africa
1979

Compiled by D. Reitmann

Readers are requested not to quote results
contained herein without first consulting
the appropriate authors.

May 1980

REPUBLIC OF SOUTH AFRICAPROGRESS REPORT TO THE INDCfor1979

Compiled by D Reitmann

1. SOUTHERN UNIVERSITIES NUCLEAR INSTITUTE, FAURE, CAPE PROVINCE

The 5.5 MV pulsed Van de Graaff accelerator at SUNI is used mainly by the Institute's own staff as well as scientists from the universities of Cape Town and Stellenbosch. The research program covers a wide variety of topics, the most relevant of which are included in this report.

1.1 Neutron reaction studies1.1.1 The structure of ^{89}Y from $(n,n'\gamma)$ measurements

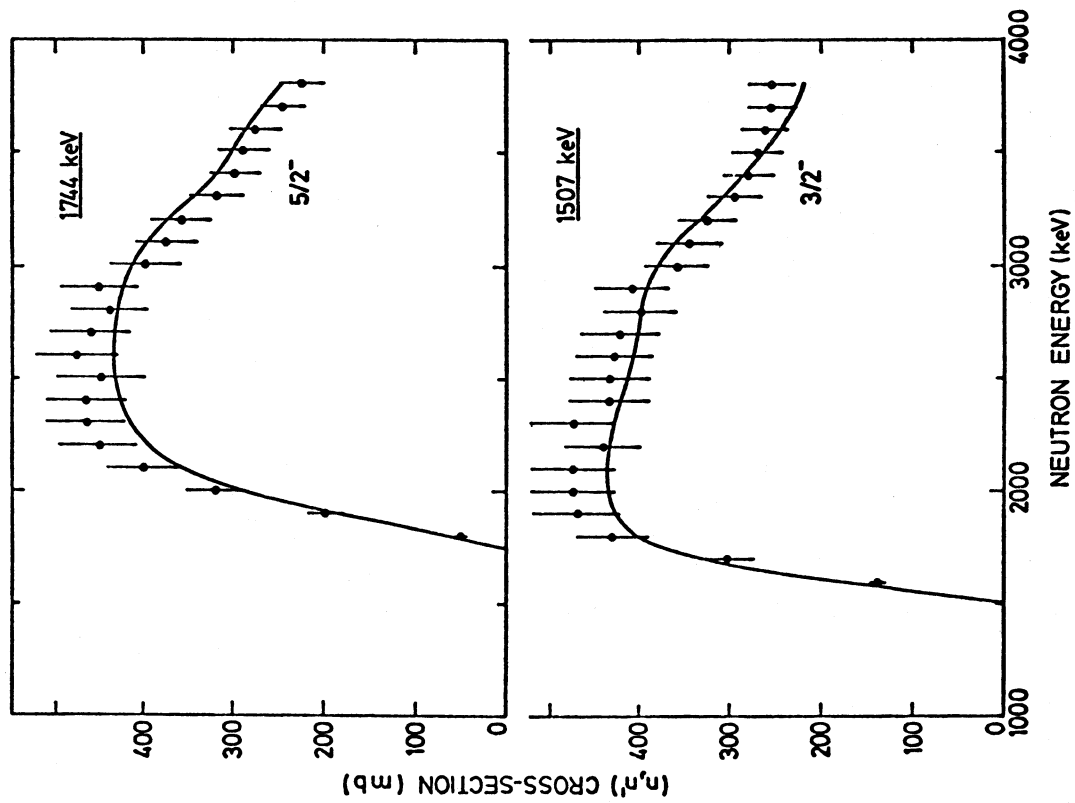
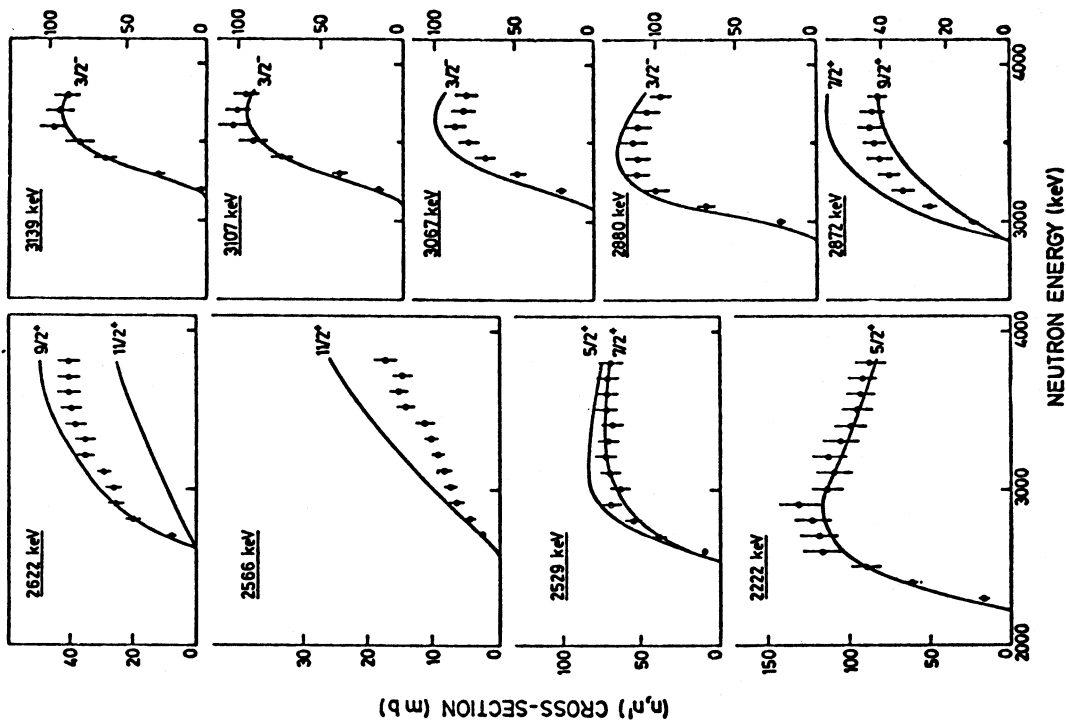
- I J van Heerden, W R McMurray, M J Renan

The study of ^{89}Y previously described¹⁾ was continued. Calculations have been completed in order to determine absolute excitation cross sections from the measured gamma-ray yields. These photon yields were corrected for incident neutron flux, γ -ray attenuation, Ge(Li) detection efficiency, the time-gate efficiency and the effect of neutron and gamma-ray attenuation in the sample. The known excitation cross section of Fe was used as a normalization standard. The data were compared with predictions of the Hauser-Feshbach model, with the aid of the computer code PELINSCA.

The results are presented in figs 1-1 and 1-2 for 11 of the excited states in ^{89}Y . J^π values are suggested in several instances where the latest published compilation²⁾ lists ambiguous or no data.

¹⁾ Item 1.1.1, SUNI Annual Research Report 1978

²⁾ D C Kocher, Nuclear Data Sheets, 16 (1975) 445



Figs. 1-1 and 1-2. Inelastic scattering cross sections for neutrons on ^{89}Y compared with Hauser-Feshbach predictions for the indicated levels of ^{89}Y .

1.1.2 The level structure of ^{115}In

- I J van Heerden and W R McMurray

Notwithstanding the large amount of experimental data on the level structure of ^{115}In , attempts to interpret these by either spherical hard-core coupling or deformed (Nilsson model) descriptions have met with mixed success.

The β -decay studies¹⁾ of ^{115}Cd and $^{115\text{m}}\text{Cd}$ and other reactions that have been studied as for example, Coulomb excitation with ^{16}O and ^{12}C ions²⁾, inelastic scattering of 12 MeV deuterons³⁾ and (d, ^3He) transfer reactions⁴⁾ such as $^{116}\text{Sn}(\text{d}, ^3\text{He})$ are all rather selective in the states excited by them. It was, therefore, decided to repeat the earlier (n,n' γ) studies of Marcinkowski⁵⁾ in an effort to locate all the energy levels and to determine their decay modes which in turn will perhaps lead to a better description of the level structure of this nucleus in terms of theoretical models. Gamma rays from levels in ^{115}In were observed following neutron scattering in the energy range 850 keV to 2500 keV in 100 keV steps. The threshold behaviour of the γ -ray intensities with increasing neutron energy, and the observed shapes of the γ -ray production excitation curves, enabled a consistent energy and decay scheme to be deduced. Fig 1-3 shows the level scheme derived from this work and those obtained from (d,d') studies³⁾, ^{115}Cd decay¹⁾, Coulomb excitation²⁾ and from the $^{116}\text{Sn}(\text{d}, ^3\text{He})$ reaction⁴⁾. Up to an excitation energy of ~1500 keV the spin and parity assignments have been reasonably well established, and these values are supported by Hauser-Feshbach calculations of the inelastic neutron scattering excitation curves.

The level observed at 1041.5 keV in these measurements decays via a 705.2 keV γ -ray to the $\frac{1}{2}^-$ level at 336.3 keV and a 444.4 keV γ -ray to the $\frac{3}{2}^-$ level at 597.1 keV. A spin assignment of $\frac{5}{2}^-$ is consistent with the decay characteristics, and this level thus probably corresponds to the 1.04 MeV level observed in the $^{116}\text{Sn}(\text{d}, ^3\text{He})$ reaction. A spin assignment of either $\frac{3}{2}^-$ or $\frac{5}{2}^-$ fits the decay data for the 1347.5 keV level, but this level has not been observed previously.

For the energy levels above 1500 keV there is a close correspondence with the levels that were observed in the inelastic scattering of 12 MeV deuterons. Because of their collective properties, it can be assumed⁶⁾ that ground state transitions from these states are predominantly E2 transitions. Table 1-1 lists the level energies and γ -ray branching ratios obtained in the various studies of this nucleus. The energy levels marked with asterisks correspond to ones also seen in the (d,d') studies³⁾. Further Hauser-Feshbach calculations will be made to place limits on the spin and parity assignments of the energy levels above 1500 keV.

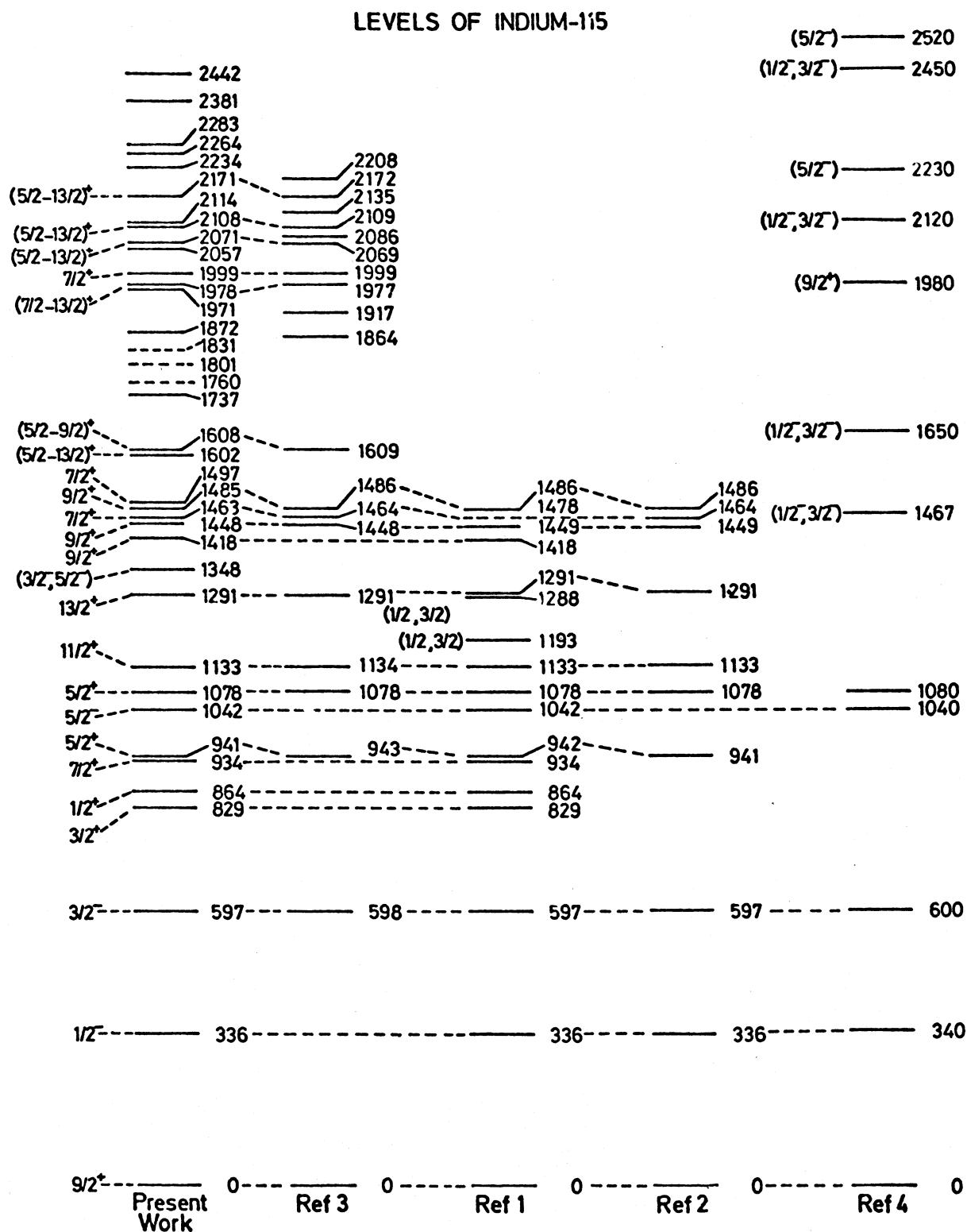


Fig. 1-3. Level schemes for ^{115}In obtained from neutron scattering (present work) and studies using other reactions¹⁻⁴).

TABLE 1-1 (Cont.)

Level (keV)	π J^π	present (n, n γ)	previous (n, n γ) (ref. 5)	$^{113}\text{Cd}^m$ and $^{113}\text{Cd}^g$ Decays (ref. 1)	($\alpha, n\gamma$) and ($^{16}\text{O}, ^{16}\text{O}_\gamma$) Coulomb Studies (ref. 3)	(5/2 - 13/2) ⁺ (7/2 ⁺)	\rightarrow 0	100	100	15	17.6
1602.3							\rightarrow 1041.5	22			
1497.2							\rightarrow 0	78			3.7
1485.3*						9/2 ⁺	\rightarrow 1132.6	15	29		78.7
							\rightarrow 941.3	85	71	85	5.8
1463.0*						7/2 ⁺	\rightarrow 1077.6	6			94.2
							\rightarrow 0	94			14.0
1448.4*						9/2 ⁺	\rightarrow 1132.6	13	12	12.6	
							\rightarrow 941.3			1.3	
							\rightarrow 933.8			0.5	
							\rightarrow 0	87	88	85.6	86.0
1418.2						9/2 ⁺	\rightarrow 1077.6			< 0.01	
							\rightarrow 941.3			< 0.1	
							\rightarrow 933.8	100	100	99.3	
							\rightarrow 0		0.6		
1347.5						(3/2, 5/2) ⁻	\rightarrow 828.6	64			
							\rightarrow 597.1	36		1.9	2.4
1290.6*						13/2 ⁺	\rightarrow 1132.6			98.1	97.6
							\rightarrow 0	100	100	100	100
1132.6*						11/2 ⁺	\rightarrow 0	100	100		1.0
1077.6*						5/2 ⁺	\rightarrow 941.3	38	43		15.6
							\rightarrow 597.1	62	57	100	83.4
							\rightarrow 0				
1041.5						5/2 ⁻	\rightarrow 597.1	12			
							\rightarrow 336.3	88		100	
941.3*						5/2 ⁺	\rightarrow 597.1	15	13	14.2	10.2
							\rightarrow 0	85	87	85.8	89.8
933.8						7/2 ⁺	\rightarrow 828.6			0.2	
							\rightarrow 0	100	100	99.8	
864.1						1/2 ⁺	\rightarrow 828.6			1.5	
							\rightarrow 597.1			0.3	
							\rightarrow 336.3	100		98.2	
828.6						3/2 ⁺	\rightarrow 597.1			8.5	
							\rightarrow 336.3	100	100	91.5	100
597.1*						3/2 ⁻	\rightarrow 336.3	100	100	100	100
336.3						1/2 ⁻	\rightarrow 0	100	100	100	100
0						9/2 ⁺	\rightarrow 0				

TABLE 1-1

LEVEL ENERGIES AND MEASURED γ -RAY BRANCHING RATIOS

Level (keV)	π J^π	Branching Ratios (in %)		
		present (n, n γ)	previous (n, n γ) (ref. 5)	$^{113}\text{Cd}^m$ and $^{113}\text{Cd}^g$ Decays (ref. 1)
2442.2		\rightarrow 0	100	
2380.6		\rightarrow 0	100	
2283.0		\rightarrow 1485.3	75	
		\rightarrow 0	25	
2264.0		\rightarrow 1347.5	65	
		\rightarrow 0	35	
2234.0		\rightarrow 0	100	
2170.7*	(5/2 - 13/2) ⁺	\rightarrow 0	100	
2113.7		\rightarrow 1132.6	88	
		\rightarrow 0	12	
2107.7*	(5/2 - 13/2) ⁺	\rightarrow 0	100	
2071.0*	(5/2 - 13/2) ⁺	\rightarrow 1418.2	34	
		\rightarrow 0	66	
2057.3		\rightarrow 0	100	
1999.0*	7/2 ⁺	\rightarrow 1418.2	23	
		\rightarrow 1041.5	47	
		\rightarrow 0	30	
1978.3*	(7/2 - 13/2) ⁺	\rightarrow 1132.6	90	
		\rightarrow 0	10	
1971.4		\rightarrow 1448.4	25	
		\rightarrow 0	75	
1872.4*		\rightarrow 1041.5	33	
		\rightarrow 933.8	67	
(1830.9)		\rightarrow 933.8	100	
(1801.0)		\rightarrow 933.8	100	
(1759.6)		\rightarrow 1132.6	100	
1736.9		\rightarrow 1418.2	24	
		\rightarrow 1132.6	39	
		\rightarrow 0	37	
1607.8*	(5/2 - 9/2) ⁺	\rightarrow 1077.6	31	
		\rightarrow 0	69	

In a recent publication¹⁾ Heyde et al. gave an alternative description of the rotational sequence of positive parity states based on the $\frac{1}{2}^+$ state at 864.1 keV by taking into account both one-hole and one-particle/two-hole configurations and by coupling these with quadrupole and octupole vibrations of the ^{116}Sn core nucleus.

- 1) K Heyde et al., Preprint UCRL-79319 (1977)
- 2) W K Tuttle et al., Phys. Rev. C13 (1976) 1036
- 3) F S Dietrich et al., Nucl. Phys. A155 (1970) 209
- 4) W H A Hesselink et al., Nucl. Phys. A226 (1974) 229
- 5) A Marcinkowski et al., Nucl. Phys. A179 (1972) 781
- 6) E Veje et al., Nucl. Phys. A109 (1968) 489

1.1.3 Levels of ^{159}Tb excited in inelastic neutron scattering

- I J van Heerden, W R McMurray, M J Renan

In terms of the Nilsson model¹⁾ most low-lying levels of a distorted odd-A nucleus such as terbium-159 can be understood as single particle states with rotational bands built on them. In addition mixing of states belonging to different major oscillator shells can also occur. A large amount of information on the level and decay scheme of ^{159}Tb has been provided by Coulomb excitation studies by Diamond et al.²⁾; by $(^3\text{He}, d)$ and (α, t) reaction studies on ^{156}Gd by Bayno et al.³⁾, and by Tippet et al.⁴⁾; and by the ^{159}Gd decay studies of Brown et al.⁵⁾. All these reactions are comparatively selective regarding the nature of the populated states, and the present $(n, n'\gamma)$ study was therefore initiated not only to reveal further energy states, but to also provide a more complete decay scheme of ^{159}Tb .

A large Ge(Li) detector was used to detect the γ -rays following inelastic neutron scattering from ^{159}Tb at several neutron energies up to 1500 keV. By courtesy of the Atomic Energy Board, Pelindaba, an intrinsic germanium detector, in a slightly modified geometry, was also used to measure the γ -rays below about 500 keV. In this geometry a 33 cm long Li_2CO_3 and paraffin shield with a tapered hole collimated the 0° neutron beam to $\pm 2^\circ$. The sample was placed immediately behind the collimator, with the detector at 90° and about 5 cm from the sample. Gamma-ray spectra recorded with this geometry and reproduced in fig 1-4 show that the γ -rays originally observed at 184 and 617 keV are in fact two doublets.

A consistent level scheme was then deduced taking into account the γ -ray threshold energies, and the shapes of the excitation curves. This level scheme is reproduced in fig 1-5. The spins and parities have been taken from

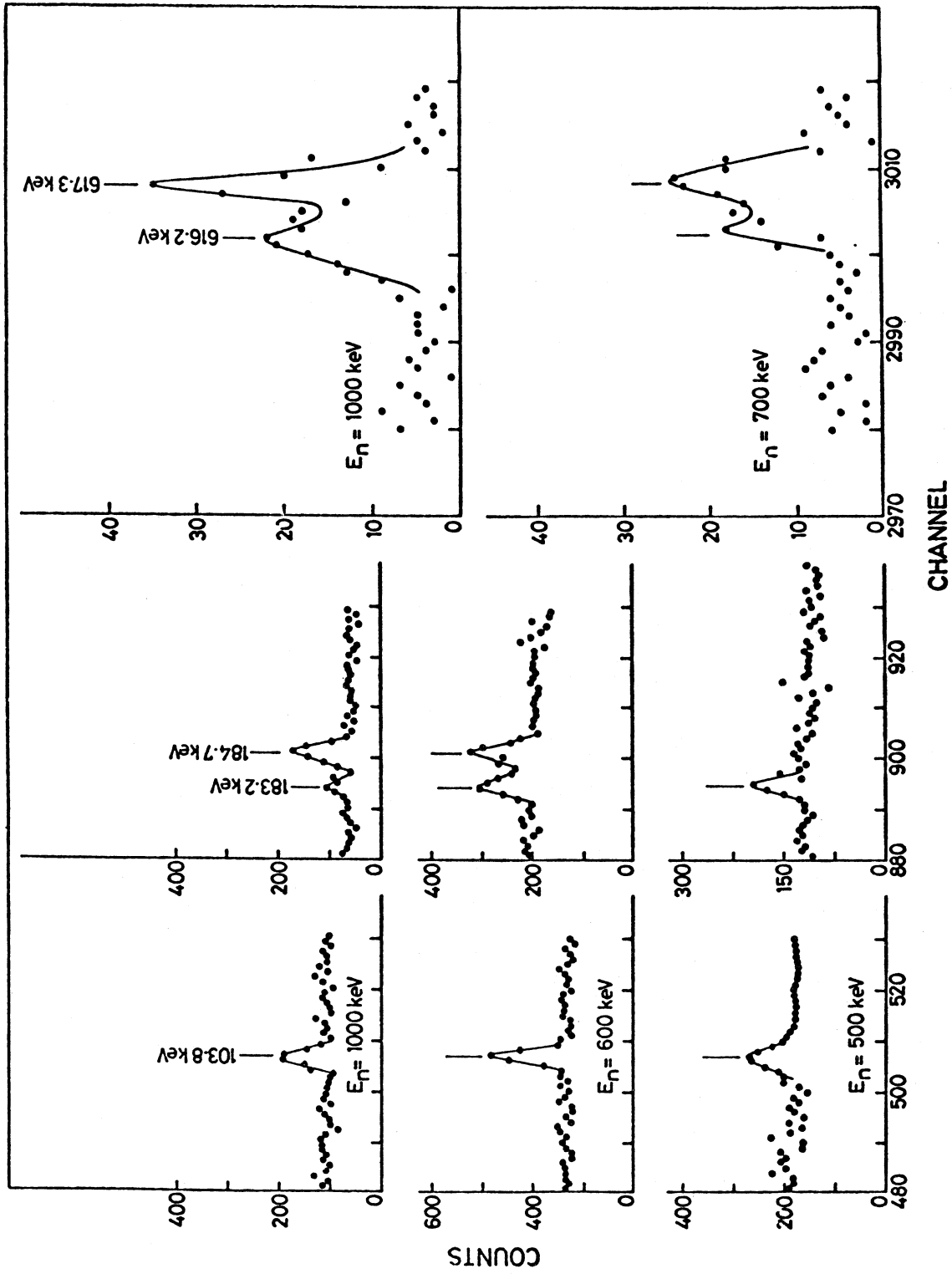


Fig. 1-4. Gamma spectra observed from $(n,n'\gamma)$ reactions on ^{159}Tb using an intrinsic germanium detector.

Fig. 1-5. The level structure of ^{159}Tb .

previous results, and are consistent with the γ -ray decays that were observed. Some inconsistencies are, however, still present. For example, if the 946.9 keV level only decayed to the $3/2^+$ ground state and to the $5/2^+$ state at 58.0 keV, it could have a spin and parity assignment of either $1/2^+$ or $3/2^-$, in agreement with previous results. It, however, also decays via a 494.1 keV γ -ray to the state at 452.8 keV tentatively assigned $9/2^-$, and might therefore be either a $5/2^-$ or a $7/2^+$ state.

The following rotational bands can be assigned on the basis of the present results:

Orbital	Level (in keV)	J^π
$3/2^+ [411]$	0	$3/2^+$
	58.0	$5/2^+$
	137.5	$7/2^+$
	241.2	$9/2^+$
$5/2^+ [413]$	348.2	$5/2^+$
	428.8	$7/2^+$
	532.9	$9/2^+$
$5/2^- [532]$	363.5	$5/2^-$
	389.5	$7/2^-$
$(3/2^+ [411] \gamma)$	580.5	$1/2^+$
$+ 1/2^+ [411]$	617.3	$3/2^+$
	674.2	$5/2^+$
	761.3	$7/2^+$
$7/2^+ [404]$	778.2	$7/2^+$
$1/2^- [541]$	854.2	$1/2^-$
	891.0	$5/2^-$

Levels with $J > 11/2$ have been observed in the Coulomb excitation work, but not in the $(n,n'\gamma)$ measurements, as could be expected. A further series of $(n,n'\gamma)$ measurements at $\theta = 125^\circ$ are now being analysed. A comparison of the excitation curves of inelastic neutron scattering cross sections with the Hauser-Feshbach predictions, corrected for level width fluctuations, will further limit the possible spins and parities of those states for which no spins and parities have been assigned, and thus will provide further insight into the systematics of the Nilsson orbitals for terbium-159.

- 1) S G Nilsson, Mat. Fys. Medd. Dan. Vid. Selsk 29 (1955)
- 2) R M Diamond et al., Nucl. Phys. 43 (1963) 560
- 3) J S Boyno et al., Phys. Rev. C6 (1972) 1411
- 4) J C Tippet et al., Can. J. Phys. 50 (1972) 3152
- 5) R A Brown et al., Can. J. Phys. 47 (1969) 1017

1.14 Anomalous behaviour of measured $^{232}\text{Th}(n,n')$ cross sections

- W R McMurray, E Barnard*, I J van Heerden, D T L Jones**

The inelastic neutron scattering cross sections for the first (49.5 keV) and second (162.5 keV) excited states of ^{232}Th as well as the elastic scattering cross sections have been carefully remeasured around the anomalies observed¹⁾ at E_n about 1000 keV. At the same time, the correspondence in the energy of the anomalies with the energy of a strong resonance in the elastic scattering of neutrons from oxygen led to a search for evidence of oxygen contamination in the sample.

Such evidence was found in the time-of-flight spectra obtained at $E_n = 1500$ and 1600 keV where the kinematics of the scattering from oxygen allows the observation of a separated oxygen peak (see fig 1-6).

More typical spectra, even those obtained close to the stronger $^{16}\text{O}(n,n)$ resonance at 440 keV, do not give unambiguous evidence for oxygen in the sample. The measurements are, however, all consistent with an oxygen content in the sample of 5.5 atom percent.

This deduced content of oxygen fully explains the anomalies in the inelastic scattering cross sections around $E_n = 1000$ keV. The kinematics of the oxygen elastic scattering causes an apparent forward-angle resonance in the scattering to the first excited state of ^{232}Th and an apparent backward-angle resonance in the scattering to the second excited state of thorium.

Our detailed measurements of the elastic and inelastic scattering of 200 - 1600 keV neutrons by the ^{232}Th nucleus²⁾ and their relevance to the level structure of ^{232}Th will now be prepared for publication.

- 1) Item 1.1.2, SUNI Annual Research Report 1978
- 2) Item 1.1.1, SUNI Annual Research Report 1976

* Atomic Energy Board, Pretoria

** National Accelerator Centre, Karl Bremer Hospital

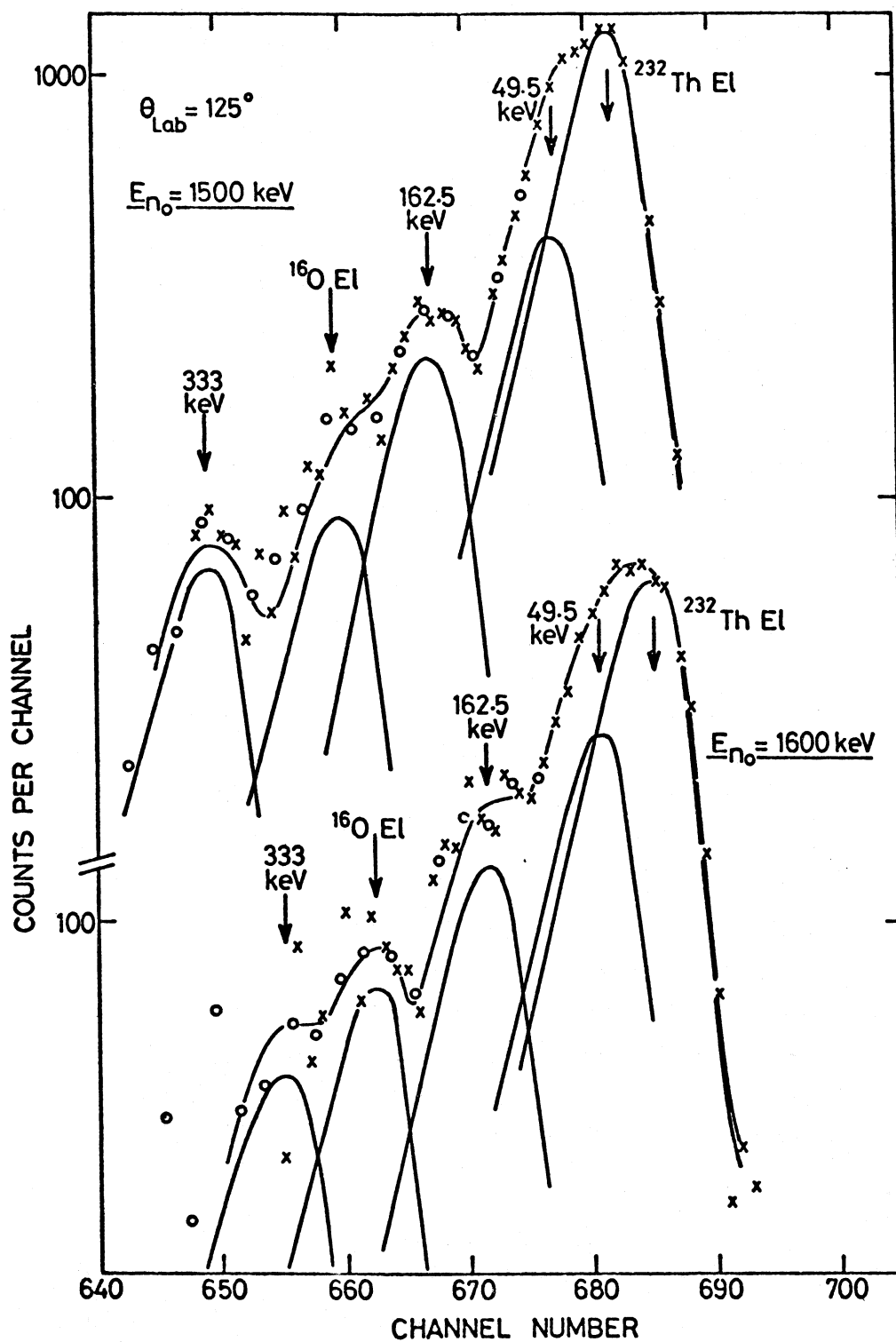


Fig. 1-6. Time-of-flight spectra of neutrons scattered from a thorium sample at $E_n = 1500$ and 1600 keV.

1.1.5 Collective band structure in levels of ^{232}Th and ^{238}U

- W R McMurray

All the available information from neutron scattering, $(n,n')^{1)}$ and $(n,n'\gamma)^{2)}$, Coulomb excitation³⁾, inelastic deuteron scattering⁴⁾ and radioactivity decay⁵⁾, has been collated in order to derive more complete information on the low-lying level structure of the two fissionable nuclei ^{232}Th and ^{238}U . These are two even-A nuclei in a region of considerable nuclear shape distortion. Their level structures, therefore, display the typical features of rotational band structure due to collective motion; ground state rotational bands, quadrupole vibrations (positive parity) and octupole vibrations (negative parity). Comparison of the deduced band structure for the positive parity levels of these nuclei shows considerable similarities (fig 1-7).

Neergaard and Vogel⁶⁾ have calculated the low-lying octupole states (negative parity) of doubly-even deformed nuclei using a microscopic description of nuclear vibrations. They achieved considerable success for a range of nuclei for which experimental information was then available. Their predictions for ^{232}Th and ^{238}U are here compared with the deductions from the present investigation (fig 1-8). It should be noted that the levels assigned to the $K = 1$ and 2 bands are not experimentally distinguishable although the sequence of spins assigns some of the levels. With this proviso it is clear that the Neergaard and Vogel calculations predict a level structure which is well reproduced by observed levels of ^{232}Th and ^{238}U . $K = 3$ octupole levels have not been experimentally identified.

The collective band assignments presented in this report have identified all the observed levels below about 1200 keV excitation with ground state rotational bands. Many higher excitation levels are observed, but these will be a mixture of intrinsic nuclear excitation and collective excitation. From the known energy for the pairing interaction (approx. 1 MeV for these nuclei) the lower lying collective levels should not be confused by intrinsic excitations.

¹⁾ E Barnard et al., Nucl. Phys. 80 (1966) 46

²⁾ W R McMurray, present work

W R McMurray, I J van Heerden, Z. Physik 253 (1972) 289

W P Poenitz, Argonne App. Phys. Ann. Report 1969/70 24

³⁾ F K McGowan et al., B A P S 16 (1971) 493

⁴⁾ T W Elze and J R Huizenga, Nucl. Phys. A187 (1972) 545

⁵⁾ G Hermann et al., Int. Conf. on properties of nuclei far from the region of β -stability II, CERN (1970) 985

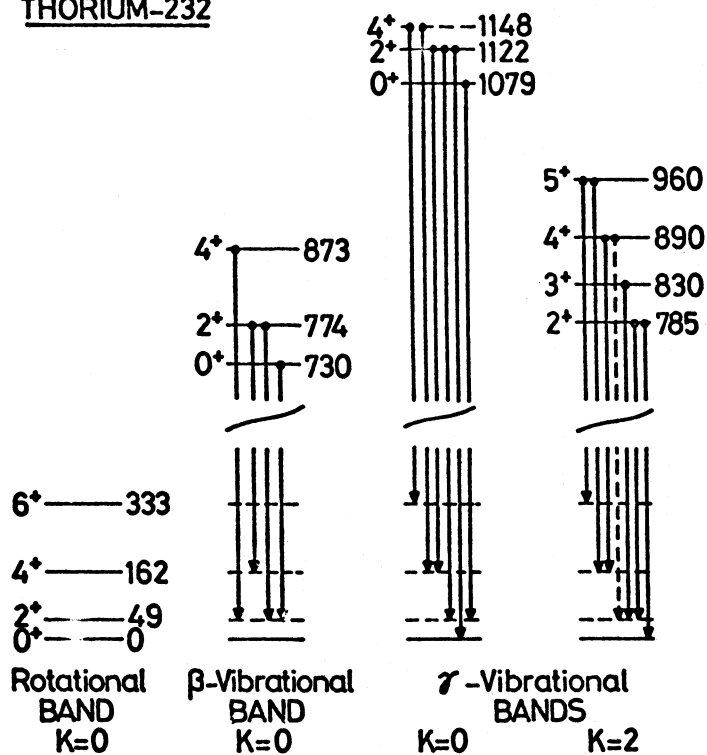
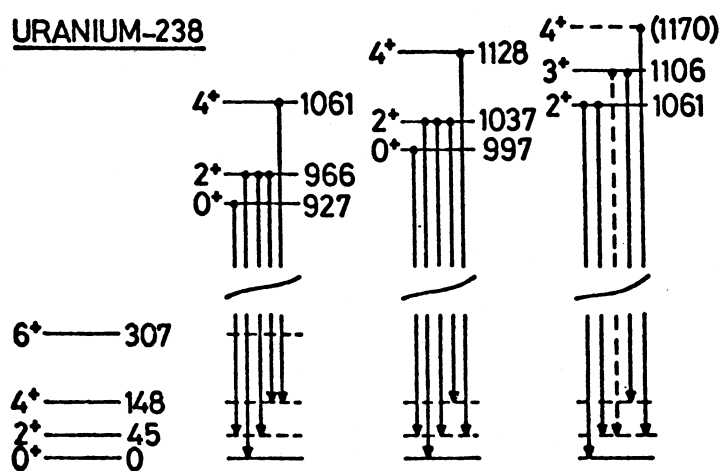
THORIUM-232URANIUM-238

Fig. 1-7. The deduced positive parity level structure of ^{232}Th and ^{238}U and the gamma decays observed in the present work.

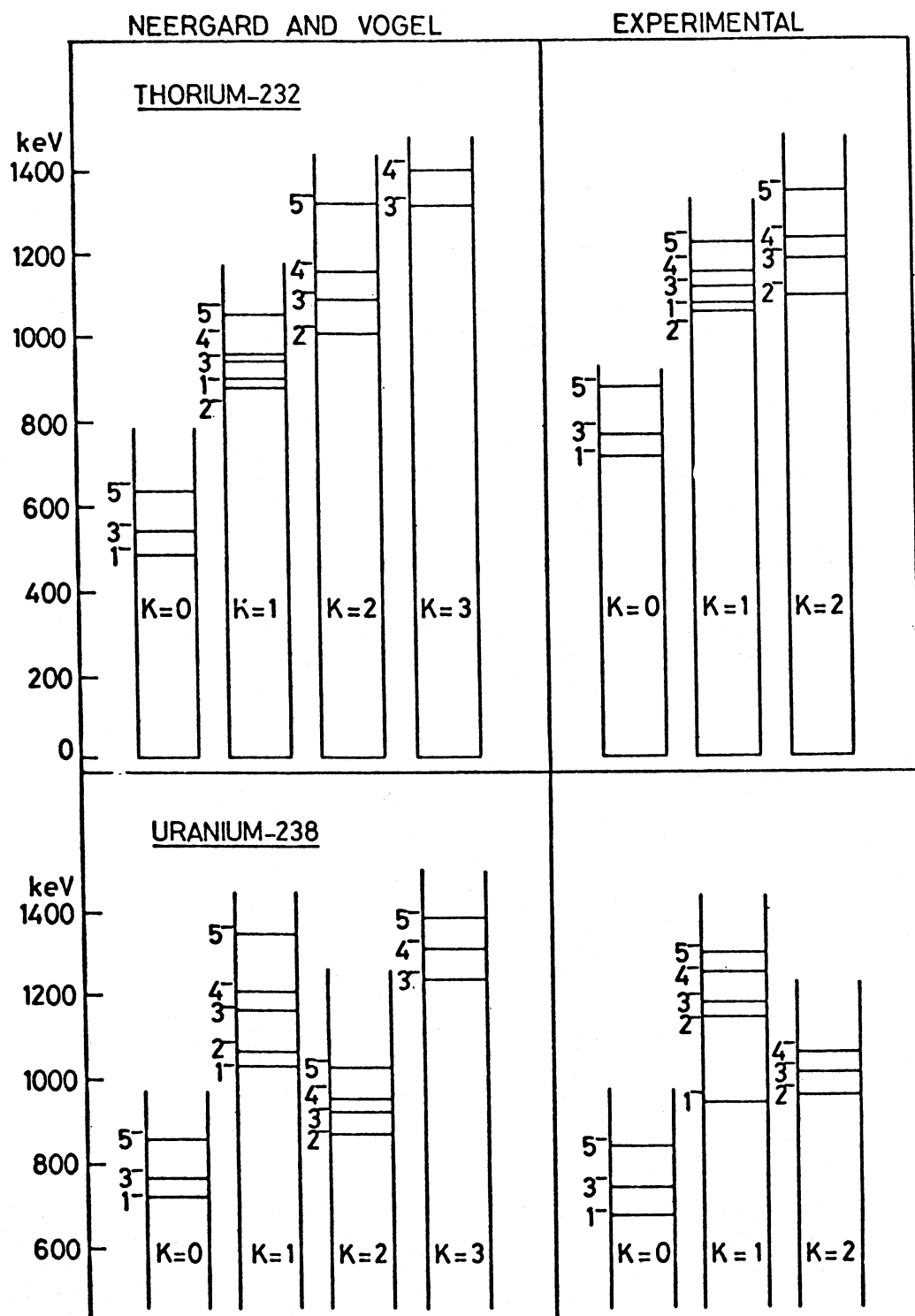


Fig. 1-8. The predicted⁶⁾ negative parity band structure of ^{232}Th and ^{238}U and the corresponding levels observed in the present study.

- ⁶⁾ K Neergard and P Vogel, Nucl. Phys. A145 (1970) 33
 Nucl. Phys. A149 (1970) 209
 Nucl. Phys. A149 (1970) 217

1.1.6 Polarization in n-p and n-d scattering at $E_n < 23$ MeV

- B R S Simpson, F D Brooks, C M Bartle, D T L Jones,
 I J van Heerden

There exists a strong motivation¹⁾ to obtain data of higher precision than is now available on the polarization in neutron-proton and neutron-deuteron scattering. With a view to achieving such precision much effort has been devoted to identifying and eliminating sources of systematic error in the anthracene and deuterated anthracene scintillation polarimeters used for these measurements at SUNI (see previous SUNI reports). In the polarimeter that has developed from these investigations, the anthracene crystal is rotated through 180° about the neutron beam at regular short intervals (typically 1 minute) and it is viewed by a pair of matched photomultipliers which remain fixed in the laboratory frame.

The rotation of the crystal is equivalent to inverting the spin state of the incident polarized neutron beam in the reference frame of the crystal. The use of two photomultipliers ensures a symmetrical laboratory arrangement, which helps to minimize systematic asymmetries introduced by rotation of the crystal. Systematic asymmetries, as determined from null polarization measurements, have been reduced to $\epsilon < 0.001$ and appear to be reducible to a lower level by further tuning of the system and by applying corrections in the data analysis. These possibilities are being explored prior to proceeding with further measurements or data reduction on the n-p or n-d polarization experiments.

¹⁾ G E Bohannon, T. Burt & P Signell, Phys. Rev. C13 (1976) 1816

1.1.7 Cross section for neutron-proton bremsstrahlung

- J Whittaker, F D Brooks, I J van Heerden

This project is now complete and the provisional result previously reported¹⁾ has been confirmed. This was an upper limit of 210 $\mu\text{b}/\text{sr}^2$ to the differential cross section for neutron-proton bremsstrahlung at 4.8 MeV incident energy, where the outgoing nucleon angles were $\theta_n = 35^\circ$, $\theta_p = 25^\circ$.

There are no directly comparable theoretical predictions; however, an estimated value of $90 \mu\text{b}/\text{sr}^2$ has been made²⁾ from elastic scattering parameters, and this is in rough agreement with extrapolations from other predictions^{3,4)} although one author³⁾ gives an alternative approach which leads to a value of $140 \mu\text{b}/\text{sr}^2$.

Whilst the measured value is unable to distinguish between these predictions, it is the most accurate result to date in the lower energy range as shown in table 1-2.

TABLE 1-2. RESULTS FROM KNOWN NEUTRON-PROTON BREMSSTRAHLUNG EXPERIMENTS
AT OR NEAR $\theta_n = \theta_p = 30^\circ$

Energy MeV	Institution	θ_n, θ_p	Cross section $d^2\sigma/d\Omega_n d\Omega_p$	Ref	Date reported
208	U C Davis	$30^\circ, 30^\circ$	$35 \pm 14 \mu\text{b}/\text{sr}^2$	⁵⁾	1968
130	Harwell	$32^\circ, 29^\circ$	$77 \pm 32 \mu\text{b}/\text{sr}^2$	⁶⁾	1974
14.4	R Boskovic Zagreb	$30^\circ, 30^\circ$	$<400 \mu\text{b}/\text{sr}^2$	⁷⁾	1970
4.8	Cape Town	$35^\circ, 25^\circ$	$60 \pm 150 \mu\text{b}/\text{sr}^2$ or $<210 \mu\text{b}/\text{sr}^2$		1979

¹⁾ Item 1.1.5 SUNI Annual Research Report (1978)

²⁾ J Whittaker, 'Neutron-proton bremsstrahlung at 4.8 MeV',
Ph.D Thesis, University of Cape Town (1979)

³⁾ J H McGuire, Phys. Rev. C1 (1970) 371

⁴⁾ M K Lion and K S Cho, Nucl. Phys. A145 (1970) 369

⁵⁾ F P Brady and J C Young, Phys. Rev. C2 (1970) 1579

⁶⁾ J A Edgington et al., Nucl. Phys. A218 (1974) 151

⁷⁾ M Furic et al., Nucl. Phys. A156 (1970) 105

1.1.8 Prompt neutrons from ^{252}Cf fission

- D M Whittal, F D Brooks, W A Cilliers

Energy measurements on two or more prompt fission neutrons which are known to have been emitted from the same fission fragment may provide information about the process of neutron emission from these highly excited nuclei. On the one hand experimental observations have been reported¹⁾ which indicate that the energies of such neutrons are uncorrelated. On the other hand, since the total initial excitation energy of each fragment is limited, the

emission of one high energy neutron should reduce the total energy available for the emission of successive neutrons from the same fragment. In other words, the energies of neutrons emitted from the same fragment might be expected to be anticorrelated, with some preference for low energy accompanying high energy.

An experiment is, therefore, being undertaken to investigate the energy-energy correlation of neutrons emitted from a spontaneously fissioning sealed ^{252}Cf source. The neutron energies are measured by time-of-flight using NE213 liquid scintillators (with PSD) to detect the fission neutrons. A cylindrical Moxon-Rae detector surrounding the ^{252}Cf source is used to determine the time of fission via the prompt fission gamma rays. The energy-energy correlation is being investigated at two neutron-neutron angles θ ; at $\theta = 30^\circ$ and $\theta = 180^\circ$. Since the fragment motion in the laboratory frame projects neutrons preferentially in the fragment directions we assume that many of the coincidences observed at $\theta = 180^\circ$ may be attributed to neutrons originating from different fragments. For the same reason we can also attribute many of the coincidences observed at $\theta = 30^\circ$ to neutrons originating from the same fragment. Thus a comparison of the energy-energy distributions observed at $\theta = 30^\circ$ and $\theta = 180^\circ$ respectively, should indicate, to a first approximation, whether a significant energy-energy correlation exists for neutrons emitted from the same fragment.

The measurement of the neutron energy-energy correlation is now in progress. Data have been acquired and the correlation analysis is about to start. Some of the data obtained at $\theta = 30^\circ$ and 180° are presented in figs 1-9 and 1-10, respectively, in the raw form in which they were acquired, that is as two-parameter distributions of the times-of-flight T_1 and T_2 of the coincident neutrons.

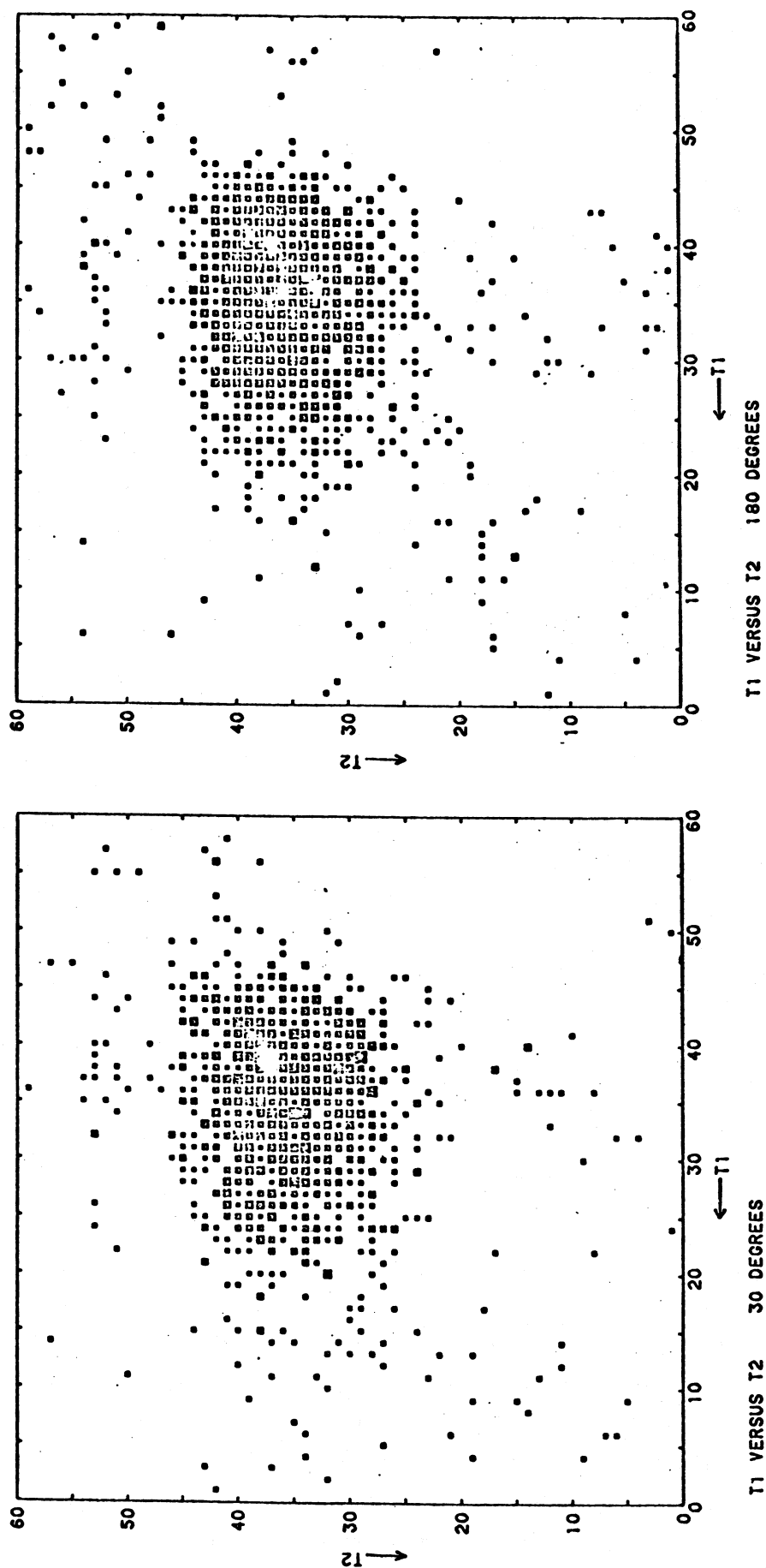
¹⁾ A Gavron and Z Fraenkel, Phys. Rev. C9 (1974) 632

1.1.9 Experiments with the associated particle neutron source

- C M Bartle, F D Brooks, D T L Jones*, W R McMurray

Monoenergetic neutron beams in the 2 to 6.5 MeV range have been produced using the associated particle neutron source. This source employs the $^2\text{H}(\text{d},\text{n})^3\text{He}$ reaction by bombarding a deuterated polyethylene target with deuterons in the 2 to 5 MeV range from the CN Van de Graaff accelerator. To extend the target lifetime the target is rotated at typically 1 rev s^{-1} with the beam directed off centre. Such a target arrangement can typically withstand up to $0.5 \mu\text{A}$ of incident deuterons focussed over a circular area of 1.6 mm diameter for several hours. The target can be periodically moved to expose a new target track on the foil.

* National Accelerator Centre, Karl Bremer Hospital



Figs. 1-9 and 1-10. Density plot showing no. of events as functions of neutron times-of-flight T_1 and T_2 for coincident neutrons emitted at relative neutron-neutron angles of $\theta = 30^\circ$ (left) and 180° (right) from the spontaneous fission of ^{252}Cf . Event-density ranges from 1 (smallest squares) to ≥ 12 (largest squares). The dispersions of the T_1 and T_2 scales are 1.1 and 1.6 ns per channel respectively.

In earlier experiments with a similar source (e.g. Bartle and Quin¹⁾), the deuterated polyethylene foil thickness was typically $100 \mu\text{g cm}^{-2}$. Using a solid state detector subtending an angle of 0.4 msr at the target, the associated neutron beam typically had a Gaussian profile with a FWHM of $3-4^\circ$, and the neutron flux within the defined beam was typically 50 s^{-1} . A calibrated beam of this order is satisfactory for cross section studies using scintillators of about 13 mm thickness which have nuclei concentrations of about $5 \times 10^{22} \text{ nuclei cm}^{-3}$ and fast neutron cross sections in the region of 50 mb or greater. The typical count rate in such a case is 2 events s^{-1} . This allows statistical accuracy of 1% in the integrated number of reaction events to be reached in approximately 2 hours. Detectors having low neutron efficiencies would require much longer counting periods so that increased neutron intensity is desirable.

In developing the SUNI source, attempts have been made to increase the usable neutron flux. Increased target thickness and increased incident deuteron current both raise the neutron beam intensity. New targets of thickness $200-400 \mu\text{g cm}^{-2}$ have been prepared by evaporating thin layers of carbon onto the two surfaces to form a sandwiched layer. These strengthened targets (first used by McFadden and Martin²⁾) have allowed target currents up to approximately $2.5 \mu\text{A}$ to be used. Consequently the neutron beam intensity which can now be achieved, is as high as 1000 s^{-1} . If an uncoated foil is bombarded with a $2 \mu\text{A}$ beam, a circular section with its perimeter corresponding to the path traced out by the beam, is cut out within a minute or so.

The preparation of thick targets is still in the development stage. The procedure used is to evaporate the first carbon layer while the foil is still on the glass slide on which it is formed (Bartle and Meyer³⁾). The foil is then floated from the slide and caught on the target holder, thus allowing the opposing carbon layer to be evaporated. The resulting foil appears to be stronger if relatively high arc voltages ($\sim 150 \text{ V}$) are employed in the evaporation. It is probable that partial melting of the foil occurs during the evaporation process. This would have the advantage that carbon is distributed throughout the foil thickness, thus improving the thermal conductivity of the foil.

Increased neutron intensity is associated with an increased elastically-scattered deuteron count-rate in the solid state detector telescope (this presently consists of a single $30 \mu\text{m}$ thick transmission detector). In preliminary experiments the detector was obviously damaged, since increases of as much as $0.4 \mu\text{A}$ in the detector leakage were observed to occur over a 24 hr period (the count rate from the detector was typically 10^6 Hz). To overcome this, a simple magnetic separating device consisting of a laboratory electro-magnet providing a 0.6 T field has been attached to a port fitted at 25° on the chamber. This achieves sufficient separation between the ^3He recoil particles

and the unwanted elastically scattered deuterons. In experiments with the magnetic analyser, recoil particle detection is restricted to 25° emission relative to the incident deuteron beam direction. For 5 MeV deuterons the associated neutron beam has a mean energy of approximately 3 MeV.

The SUNI associated particle source has been employed in studies of reactions on ^{40}Ca and ^6Li . These experiments were in the main conducted with low intensity neutron beams (without the analyser) since the over-riding considerations were reduced gross count-rate in the scintillator and flexibility in the kinematic selection of the neutron energy. Cross sections have been measured for the $^{40}\text{Ca}(n,p)$ and $^{40}\text{Ca}(n,\alpha)$ reactions in the energy range $E_n = 5$ to 6.5 MeV. The data are in the analysis stage.

Fig 1-11 shows the present status of $^{40}\text{Ca}(n,\alpha_0)$ data and recent Hauser-Feshbach⁴⁾ calculations with (Fu(2)) and without (Fu(1)) width-fluctuation corrections. The agreement between Fu(2) and the data appears good, but considerable uncertainty in the experimental values in the region of 6 MeV remains. It is hoped that the SUNI data will improve knowledge of the cross section at these higher energies. The experimental $^{40}\text{Ca}(n,p_{0,1,2,3})$ cross sections also shown in fig 1-11 are much lower than the calculated values.

Studies are also in progress on the $^6\text{Li}(n,nd)^4\text{He}$ reaction. This can be observed as a broad peak at low pulse heights when fast neutrons bombard a $^6\text{LiI}(\text{Eu})$ scintillator. Interest in this reaction arises primarily from its relationship to the $^7\text{Li}(n,nt)^4\text{He}$ reaction of importance in the breeding cycle of the proposed fast breeder reactors. The cross section in the 3-14 MeV range is known only to $\pm 20\%$ which is too poor for reliable calculations in the fusion reactor program. Improvements can probably be effected, based on the "raw" $^6\text{LiI}(\text{Eu})$ data, but it is difficult to reliably separate $^6\text{Li}(n,nd)^4\text{He}$, and $^{127}\text{I}(n,n\gamma)^{127}\text{I}$ events. Attempts have been made to achieve separation using pulse shape discrimination. Such discrimination has not been achieved at room temperature but may prove possible at low temperatures.

- 1) Bartle and Quin, Nucl. Instr. & Meth. 121 (1974) 119
- 2) McFadden and Martin, Nucl. Instr. & Meth. 113 (1973) 601
- 3) Bartle and Meyer, Nucl. Instr. & Meth. 112 (1973) 615
- 4) Fu(1979) private communication, see also Atom. Data and Nucl. Data Tab. 17 (1976) 127
- 5) Bartle, Johnson and Chapman, Nucl. Phys. A220 (1974) 395

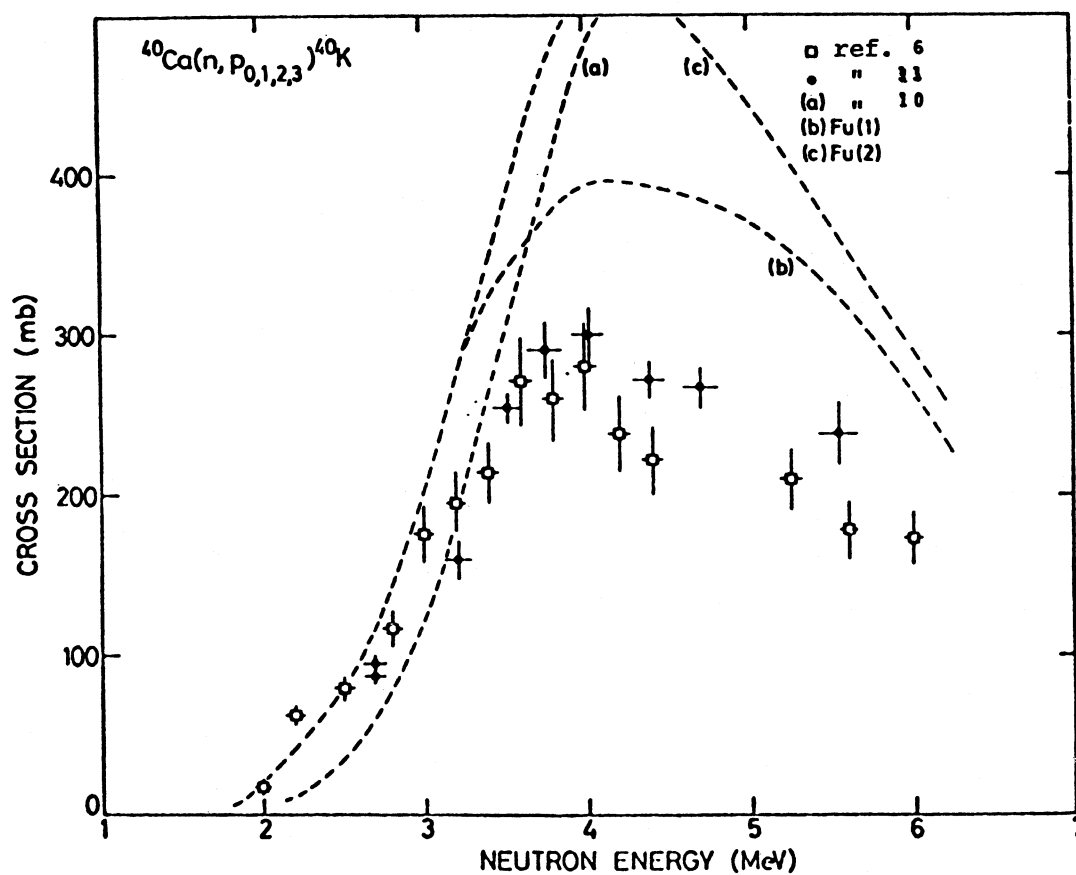
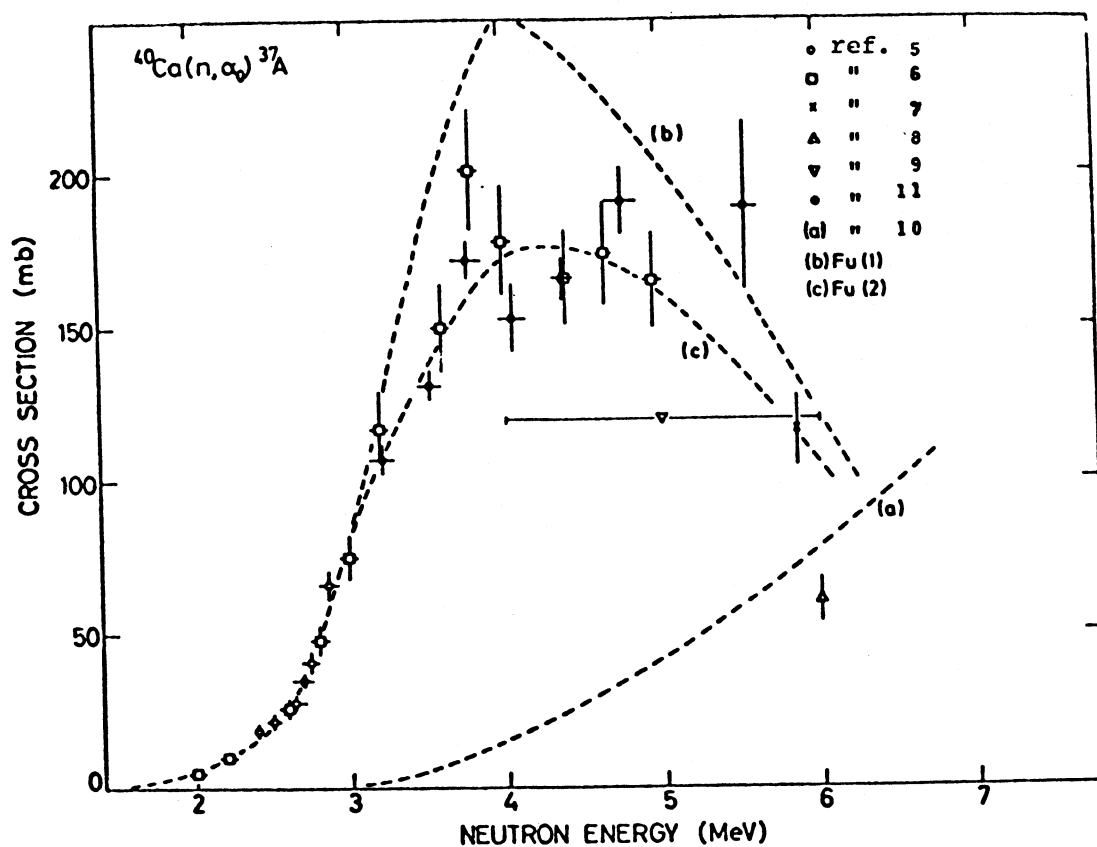


Fig. 1-11. Comparison between various measurements of the $^{40}\text{Ca}(n, \alpha_0)$ and $^{40}\text{Ca}(n, p_{0,1,2,3})$ reactions and Hauser Feshbach predictions.

- ⁶⁾ Bass and Saleh, EANC(D)66"U", p.64, CINDA, Vienna
- ⁷⁾ Foroughi and Rossel, Helv. Phys. Acta. 34 (1962) 439
- ⁸⁾ Knellwolf and Rossel, Helv. Phys. Acta. 39 (1966) 376
- ⁹⁾ Viennet, Knellwolf and Rossel, Helv. Phys. Acta. 37 (1964) 222
- ¹⁰⁾ Pearlstein, Journ. Nucl. En. 27 (1973) 811
- ¹¹⁾ Bartle and Quin (1972) unpublished

1.1.10 Neutron flux monitor

- C M Bartle and D M Whittall

Cross section measurements for the $^{23}\text{Na}(n,p)$ and $^{23}\text{Na}(n,\alpha)$ reactions, have been obtained over a wide range of energies^{1,2)}. Conversely the yield of protons and alphas from these reactions in a known energy spectrum of neutrons enables the flux to be determined.

This technique has been used in the measurement of the flux from a number of Am-Be neutron sources using a NaI(Tl) detector. From the known shape of the neutron energy spectrum and the cross section versus energy dependence, a mean value for the reaction cross sections have been calculated.

The (n,p), (n, α) and gamma-ray events which occur in the inorganic scintillator NaI(Tl) when it is placed in a mixed radiation field have been distinguished from one another by utilising the pulse shape discrimination properties of the scintillator¹⁾.

The method has been tested by obtaining PSD spectra from Am- α -Be sources of various strengths. In each case, the calculated neutron flux compared favourably with the manufacturer's specifications.

- ¹⁾ C M Bartle, Nucl. Instr. & Meth. 124 (1975) 547
- ²⁾ C F Williamson, Phys. Rev. 122 (1961) 1877

1.1.11 Study of (d,n) and (^3He ,n) reactions

- F D Brooks, B R S Simpson, W R McMurray, I J van Heerden,
D T L Jones*

A study is in progress of (d,n) reactions on some target nuclei in the 1p, 1d_{2s} and 1f_{2p} shells and preparations are in hand to study (^3He ,n) reactions on targets in the same mass region. The objective is to obtain spectroscopic information on the proton-rich product nuclei of these reactions. The reactions

* National Accelerator Centre, Karl Bremer Hospital

are being investigated using a new type of neutron spectrometer¹⁾ in which the neutron spectrum is derived directly from the pulse height and pulse shape information recorded by a deuterated anthracene scintillator.

The $^{19}\text{F}(\text{d},\text{n})^{20}\text{Ne}$ reaction ($Q_{\text{gs}} = 10.6$ MeV) has been studied at SUNI using 5.0 MeV incident deuterons from the SUNI CN Van de Graaff. The $^{12}\text{C}(\vec{\text{d}},\text{n})^{13}\text{N}$, $^{28}\text{Si}(\vec{\text{d}},\text{n})^{29}\text{P}$ and $^9\text{Be}(\vec{\text{d}},\text{n})^{10}\text{B}$ reactions ($Q_{\text{gs}} = -0.26, 0.52$ and 4.36 MeV respectively) have been studied in collaboration with J M Nelson, P M Lister and K S Dhuga of the University of Birmingham, using the 12.3 MeV vector-polarized deuteron beam of the Birmingham Radial Ridge Cyclotron. Some neutron spectra obtained from the $(\vec{\text{d}},\text{n})$ reactions on ^{28}Si and ^9Be are shown in fig 1-12. In each case the spectra obtained simultaneously for the "up" state and the "down" state of the polarized incident beam are shown and arrows indicate the expected positions of peaks corresponding to transitions to different energy levels in ^{29}P and ^{10}B respectively. The energy resolution of the neutron spectrometer was about 250 keV (FWHM) at 10 MeV in these measurements.

Some vector analysing power (VAP) data obtained from the measurements of the $^{12}\text{C}(\vec{\text{d}},\text{n})^{13}\text{N}$ and $^{28}\text{Si}(\vec{\text{d}},\text{n})^{29}\text{P}$ reactions are shown in figs 1-13 and 1-14. The VAP data for the $\ell = 1, j = \frac{1}{2}$ transition to the ground state of ^{13}N (fig 1-14) agree well with the DWBA prediction shown. The $\ell = 2, j = \ell + \frac{1}{2} = 3/2$ or $5/2$ transitions to the 1.38 and 1.96 MeV levels respectively of ^{29}P (fig 1-14) show the mirror-like j -dependence of the VAP angular distributions at forward angles. Thus the features observed in these proton transfer reactions follow the well-known pattern found in neutron transfer $(\vec{\text{d}},\text{p})$ reactions. This, in turn, helps to establish the validity of VAP measurements as a spectroscopic tool for assigning j -values to energy levels of the product nuclei formed in $(\vec{\text{d}},\text{n})$ reactions.

¹⁾ Item 1.1.8, SUNI Annual Research Report 1978

1.1.12 Measurements of (n,p) and (n,d) reactions with 22 MeV neutrons

- W R McMurray, K Bharuth-Ram*, C M Bartle, S M Perez, F D Brooks

A technique¹⁾ has been developed to observe low cross section (n,p) and (n,d) reactions at $E_n = 22$ MeV. This work was specifically undertaken to observe the analogue of the giant dipole resonance (GDR) in ^{90}Zr in the proton energy spectrum from (n,p) reactions going to excited states of ^{90}Y . For the $^{90}\text{Zr}(\text{n},\text{p})^{90}\text{Y}$ reaction at $E_n = 22$ MeV the analogue is expected to appear in an enhanced proton yield in the range 10-19 MeV (as deduced from the excitation

* University of Durban-Westville, Durban

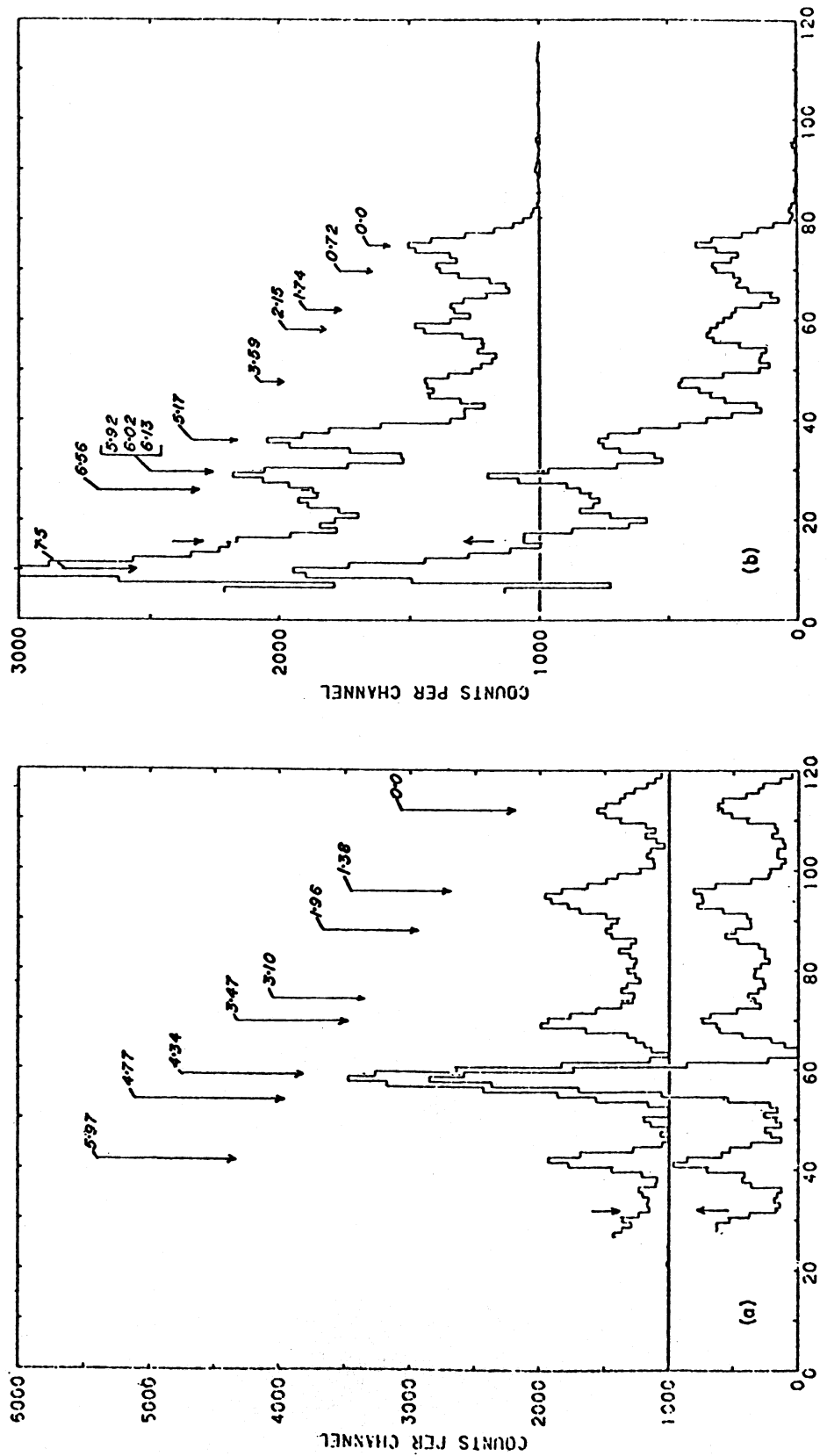


Fig. 1-12. Neutron spectra obtained from: (a) $^{28}\text{Si}(\vec{d}, n)^{29}\text{P}$ reaction at $\theta = 85^\circ$; and (b) $^9\text{Be}(\vec{d}, n)^{10}\text{B}$ reaction at $\theta = 85^\circ$. The lower and upper spectra correspond to the spin "up" and spin "down" states respectively of the vector polarized incident deuteron beam (12.3 MeV). A continuum background corresponding to the neutron spectrum from deuteron breakup has been subtracted from spectra (a).

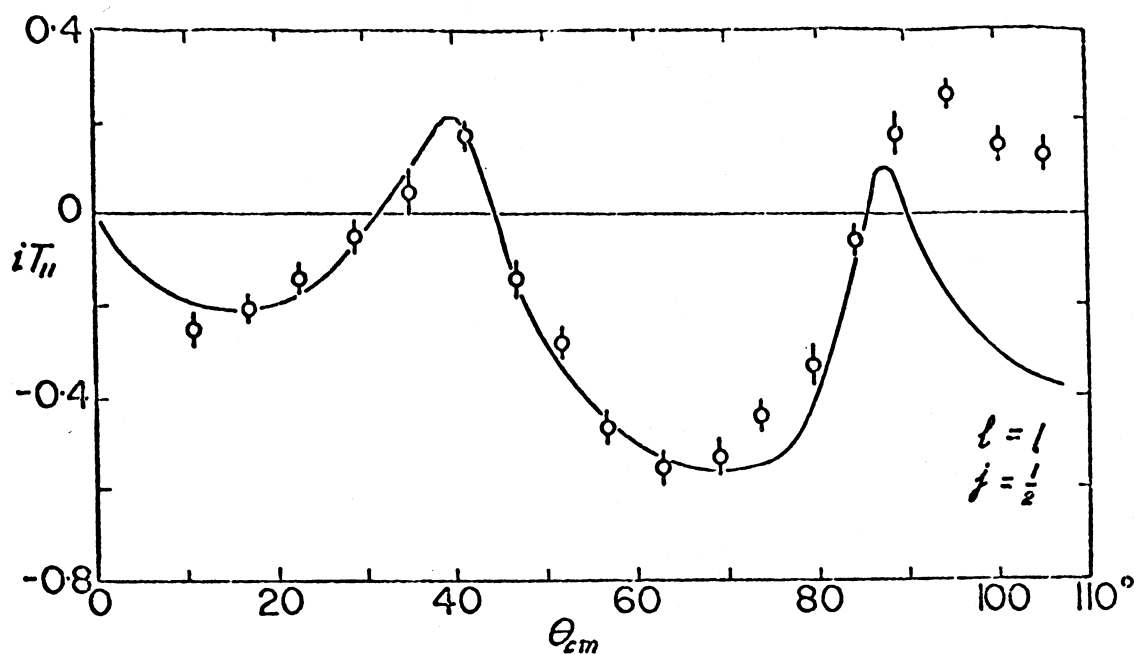


Fig. 1-13. Vector analysing power for the ground state transition in the $^{12}\text{C}(d,n)^{13}\text{N}$ reaction. The curve shows the VAP calculated from DWBA theory.

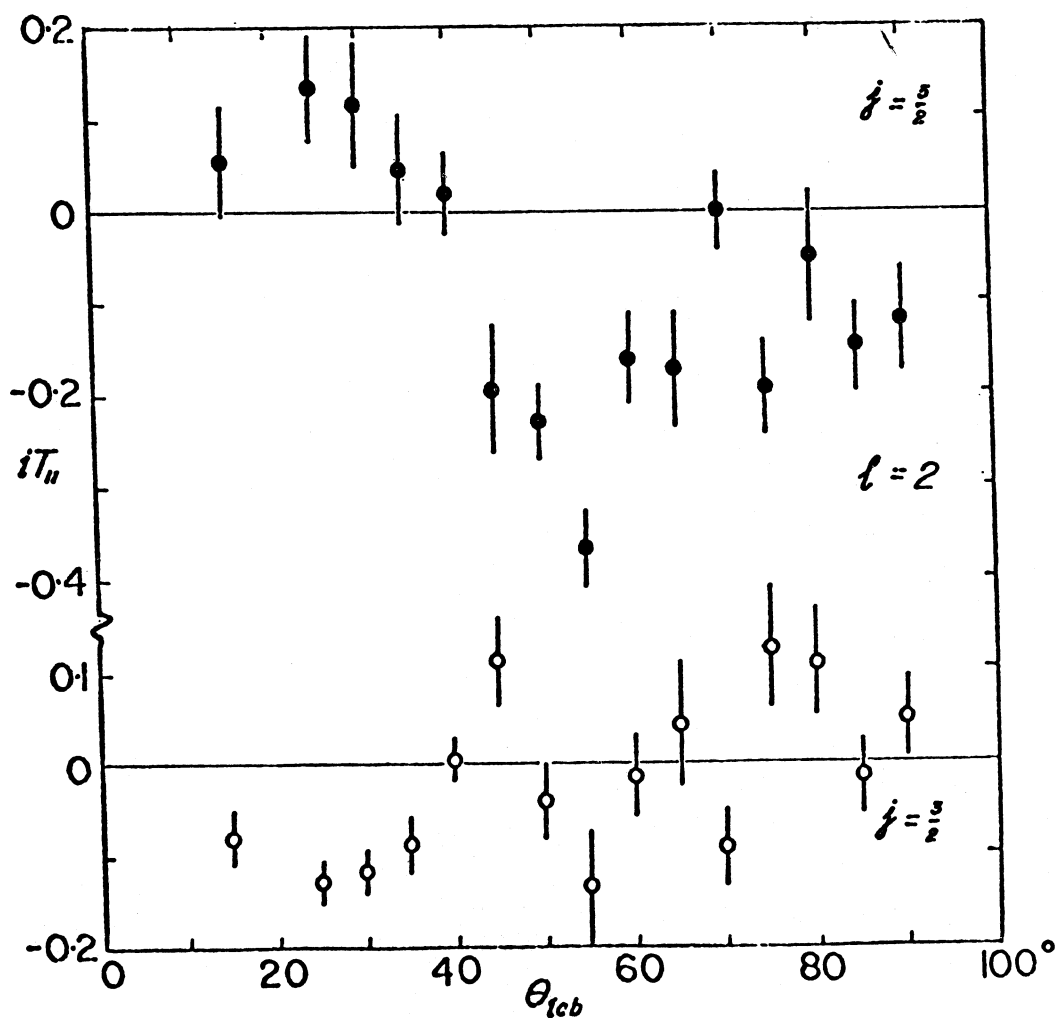


Fig. 1-14. Vector analysing powers for the transitions leading to the 1.38 MeV level (open circles) and the 1.96 MeV level (solid circles) of ^{29}P in the $^{28}\text{Si}(d,n)^{29}\text{P}$ reaction.

of the GDR in ^{90}Zr and the Coulomb energy difference between ^{90}Zr and ^{90}Y). Theoretical treatment²⁾ of the excitation of the analogue of the GDR has been used by Perez to obtain angular distribution of the cross section. The direct reaction process leads to a forward peaked angular distribution shape.

Previous measurements¹⁾ gave qualitative evidence for the excitation of the analogue of the GDR in the $^{90}\text{Zr}(n,p)^{90}\text{Y}$ reaction. Quantitative support for the theory of Clements and Perez²⁾ could not then be obtained because no obvious method was available for assessing the "compound-nuclear" background leading to proton emission in the 10-20 MeV energy range as a function of proton emission angle.

Two approaches to the determination of this background have been made

- (i) proton energy spectra from the $^{56}\text{Fe}(n,p)^{56}\text{Mn}$ reaction have been observed as a function of angle for the same range of proton energies and
- (ii) measurements for the $^{90}\text{Zr}(n,p)^{90}\text{Y}$ and $^{56}\text{Fe}(n,p)^{56}\text{Mn}$ reactions have been extended to larger angles ($\theta_{\text{max}} = 75^\circ$).

The $^{56}\text{Fe}(n,p)$ reaction at proton energies above about 12 MeV should not be complicated by analogue excitations (expected for $E_p \sim 5$ to 12 MeV). The results show that the $^{56}\text{Fe}(n,p)$ reaction leads to a nearly isotropic reaction cross section for $E_p > 12$ MeV and the $^{90}\text{Zr}(n,p)$ reaction cross sections tend towards the $^{56}\text{Fe}(n,p)$ cross sections at large angles $\theta = 65^\circ$. Quantitative analysis of the accumulated data is nearly complete. Preliminary results are in rough agreement with the theory of Clements and Perez²⁾.

¹⁾ Item 1.1.6, SUNI Annual Research Report (1978)

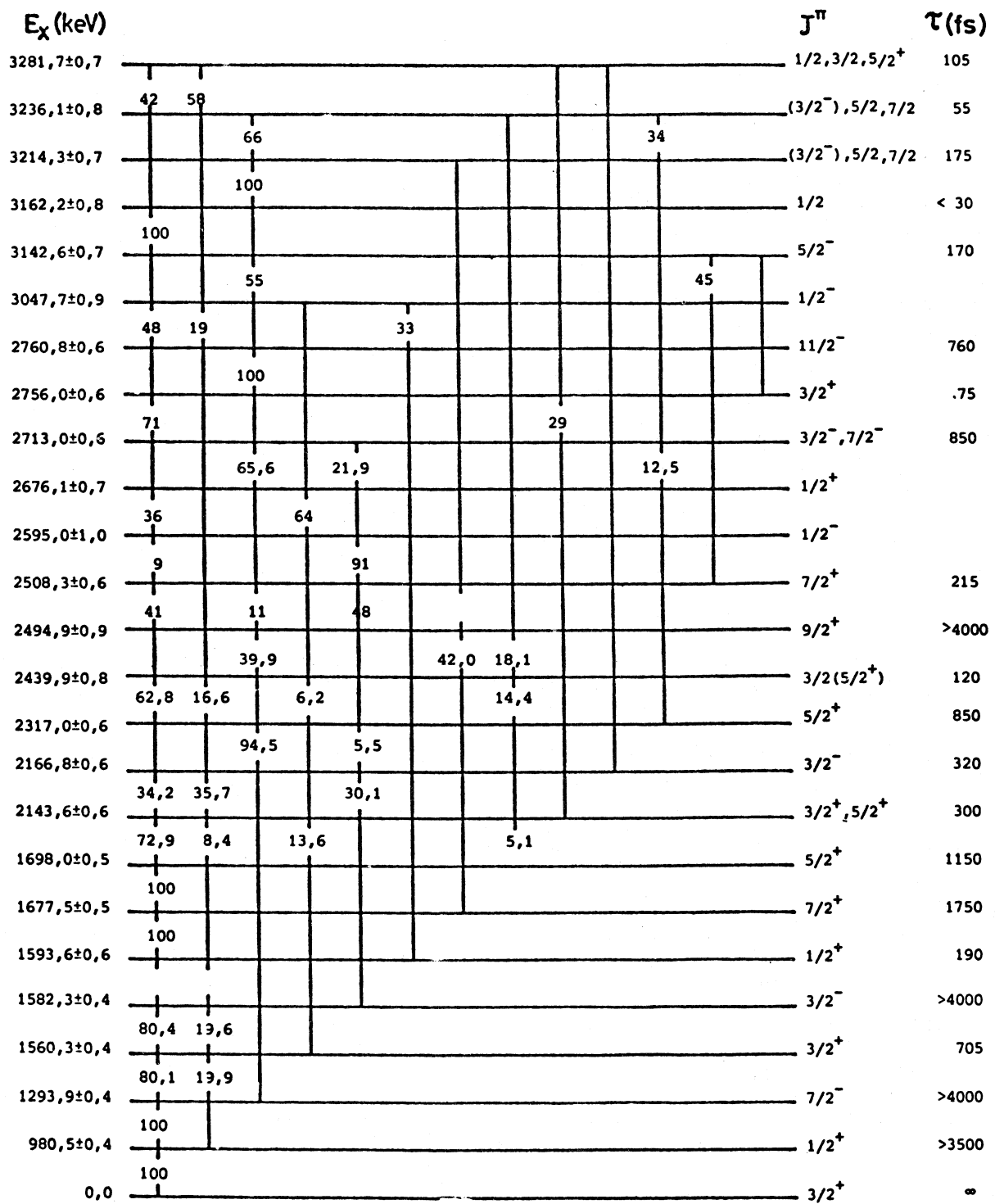
²⁾ C F Clements and S M Perez, Nucl. Phys. A165 (1971) 569

1.2 Charged particle reaction studies

1.2.1 Electromagnetic properties and spins of states in ^{39}K and ^{41}K

- J A Stander, W J Naudé, N J A Rust, J W Koen

Preliminary results on the energies, decay properties and lifetimes of levels in these nuclei and studies of spin values using Hauser-Feshbach theory, have been reported previously^{1,2)}. This investigation has now been completed and the results have been discussed in the Ph.D thesis of J A Stander, together with the results of angular correlation measurements using Litherland-Ferguson Method II and the $^{36}\text{Ar}(\alpha, p\gamma)^{39}\text{K}$ reaction³⁾.

Fig. 1-15. Properties of energy levels in ^{41}K .

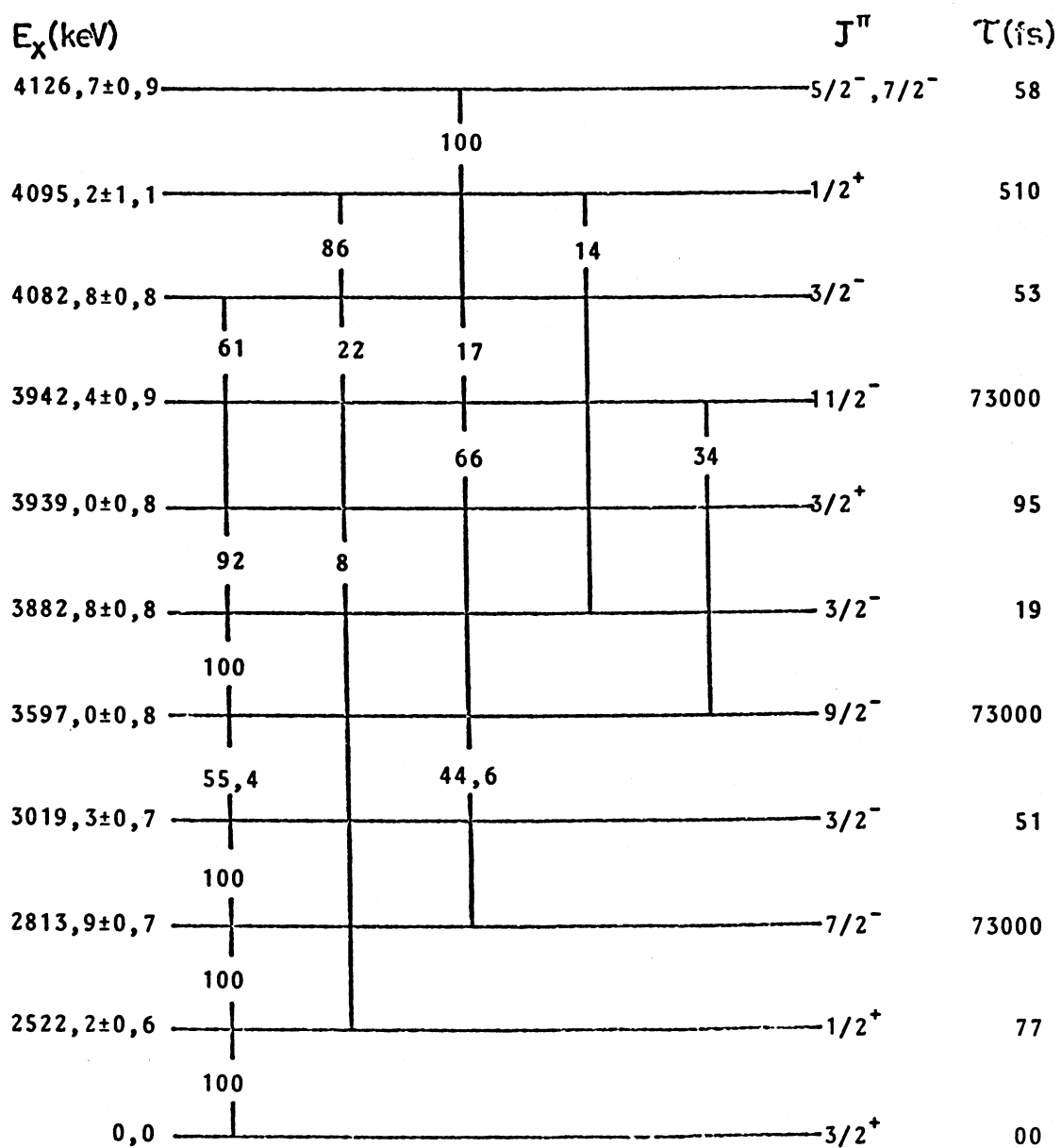
Fig. 1-16. Properties of energy levels in ^{39}K .

TABLE 1-3 MIXING RATIOS FOR TRANSITIONS TO THE GROUND STATE IN ^{39}K

TRANSITION (MeV) $E_i \rightarrow E_f$	$J_i^\pi \rightarrow J_f^\pi$	RADIATION	MIXING RATIO						
			THIS STUDY	No 75	Ma 70	Pe 70	Fr 77	Lo 68	Eg 78
2,522+0	$1/2^+ \rightarrow 3/2^+$	M1/E2	ISOTROPIC	-	-	$\pm 0,94 \pm 0,17$	$\pm 0,63 \pm 0,09$	-	-
2,814+0	$7/2^- \rightarrow 3/2^+$	M2/E3	$-0,16 \pm 0,03$	$-0,14 \pm 0,02$	-	$\pm 0,20 \pm 0,02$	-	$-0,19 \pm 0,10$	$-0,16 \pm 0,02$
3,019+0	$3/2^- \rightarrow 3/2^+$	E1/M2	$-0,04 \pm 0,07$	-	$-0,02 \pm 0,04$	-	-	$-0,03 \pm 0,15$	-
3,597+0	$9/2^- \rightarrow 3/2^+$	E3/M4	0 $\pm 0,06$	-	-	-	-	-	-
3,883+0	$3/2^- \rightarrow 3/2^+$ $5/2^- \rightarrow 3/2^+$	E1/M2 E1/M2	$0,12 \pm 0,10$ $-0,27 \pm 0,07$	- -	- -	- -	- -	- -	- -
3,939+0	$1/2^+ \rightarrow 3/2^-$ $3/2^+ \rightarrow 3/2^+$ $5/2^+ \rightarrow 3/2^+$	M1/E2 M1/E2 M1/E2	ISOTROPIC $0,05 \pm 0,20$ $-0,38 \pm 0,18$	- - -	- - -	- - -	- - -	- - -	- - -
4,083+0	$3/2^- \rightarrow 3/2^+$	E1/M2	$-0,06 \pm 0,11$	-	-	-	-	-	-

No 75: Nolan et al., J Phys G1 (1975) L33

Ma 70: S Maripuu, Nucl Phys A151 (1970) 465

Pe 70: Peterson et al., Nucl Phys A143 (1970) 337

Fr 77: Frey et al., Proc Tokyo Conf (1977) p172

Lo 68: Lopes et al., Nucl Phys A109 (1968) 241

Eg 78: Eggehuisen et al., Nucl Phys A305 (1978) 245

The results are summarised in figs 1-15 and 1-16 and in table 1-3 for excitation energies up to 4127 keV in ^{39}K and 3282 keV in ^{41}K . In table 1-3 the spin possibility of $5/2^-$ for the 3,883 MeV level is unacceptable in view of the too large M2 enhancement. ($\delta = -0,27 \ 0,07$). For the 3,939 MeV level the Hauser-Feshbach analysis indicates $J^\pi = 3/2^+$ on the basis of both the total $^{39}\text{K}(p,p')^{39}\text{K}$ cross section and the (p,p') angular distribution measured at incident proton energies of about 6 MeV.

- 1) Item 1.2.1, SUNI Annual Research Report (1978)
- 2) Item 1.2.3, SUNI Annual Research Report (1977)
- 3) Item 1.2.4, SUNI Annual Research Report (1978)

1.2.2 Shell model calculations of ^{39}K and ^{41}K

- J A Stander, W J Naudé, R Saayman

Experimental values of energy level schemes, static moments and electromagnetic transition probabilities (see section 1.2.1) were compared with predictions of the many particle shell model using an effective surface delta interaction. A full description is given in the thesis of J A Stander.

For ^{39}K an inactive ^{28}Si -core was assumed with eleven nucleons occupying the $1s_{1/2}$ and $0d_{3/2}$ subshells with allowance for particle evacuation of the $1s_{1/2}$ and single particle excitations of either the $0f_{7/2}$ or $1p_{3/2}$ subshells. The two isobaric analogue states $T = 3/2$; $J = 7/2^-$, $3/2^-$ corresponding to the ground and first excited state of ^{39}Ar respectively were included in the calculations whereas the ground state of $^{39}\text{K}(3/2^+)$ and first excited state $(1/2^+)$ were assumed to be $(0d_{3/2})^{-1}$ and $(1s_{1/2})^{-1}$ proton holes in a closed ^{40}Ca -core.

The calculated energy levels in fig 1-17 compare favourably with experiment and the Tamm-Dancoff calculations of Hsieh et al.¹⁾, if it is taken into account that the spin of the 3,883 MeV level is probably $3/2^-$ rather than $5/2^-$ as assumed by Hsieh et al. The calculated static moments and transition probabilities are similarly in acceptable agreement with experiment.

In view of the relatively small contribution of $1s_{1/2}$ excitation to the calculated level scheme of ^{39}K , a ^{32}S -core was assumed for ^{41}K calculations with even and odd parity shapes described in terms of $0d_{3/2}^7 \ 0f_{7/2}^2$ and $0d_{3/2}^6 \ 0f_{7/2}^3$ configurations respectively. Considering the relatively small size of the shell model space and the large number of experimental energy levels over a small energy range, the agreement obtained between theory and experiment was reasonable.

¹⁾ S T Hsieh, K T Knöpfle, G J Wagner, Nucl. Phys. A254 (1975) 141

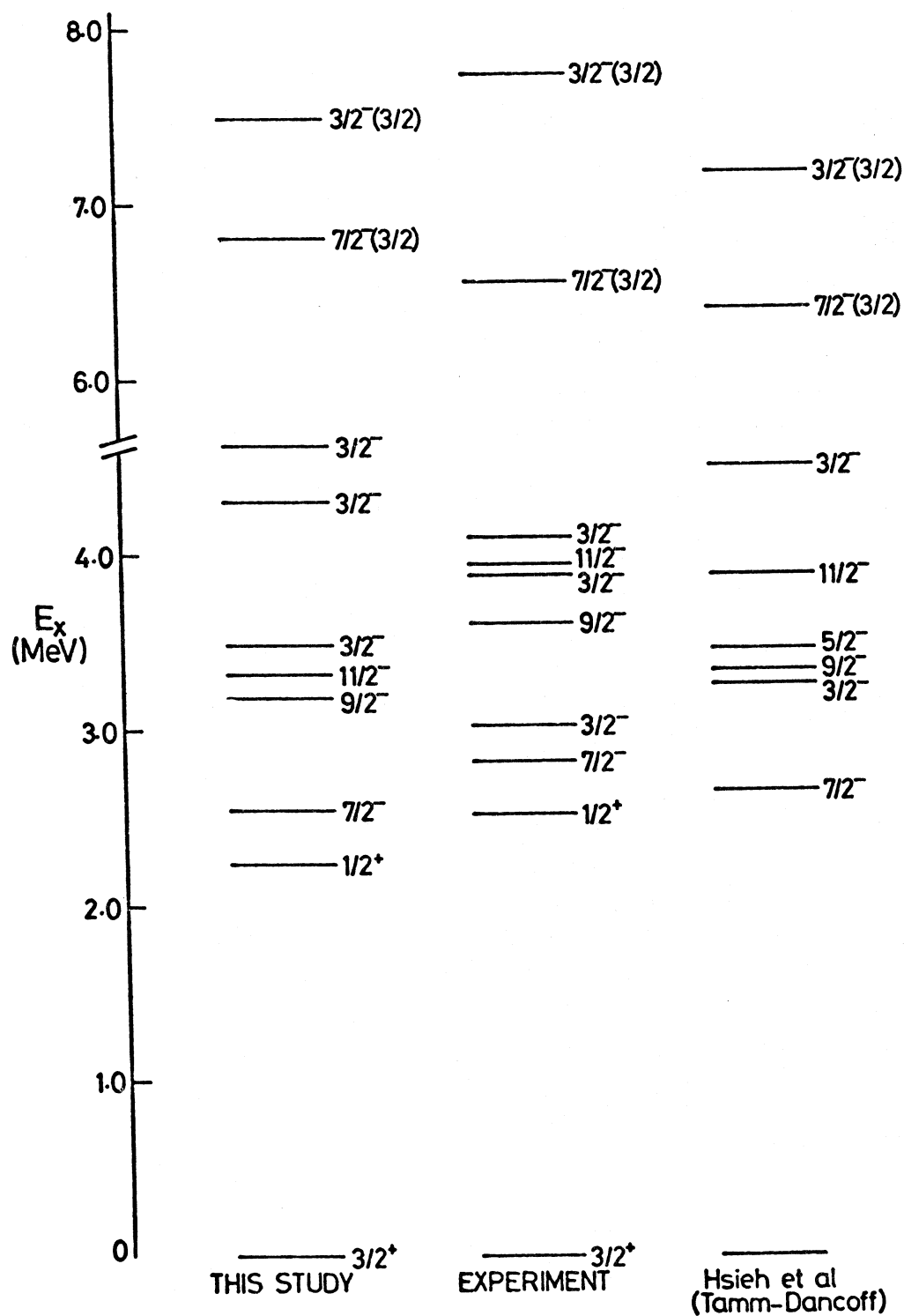


Fig. 1-17. Comparison of calculated and experimental level schemes for ^{39}K .

1.2.3 Properties of energy levels in ^{54}Cr

- F D Smit, N J A Rust, W J Naudé, J W Koen

The $^{51}\text{V}(\alpha, p\gamma)^{54}\text{Cr}$ reaction was used to investigate the level scheme and decay properties of levels up to 4 MeV excitation in ^{54}Cr . A doubly ionized $^4\text{He}^{++}$ beam with an energy of about 12 MeV was employed.

The level energies, branching ratios and mean lifetimes were determined with a single experimental arrangement using a $\Delta E - E$ telescope to detect protons from the reaction and two Ge(Li) detectors at different angles for gamma detection. The telescope was placed at 120° with respect to the incident beam and consisted of a $200\ \mu\text{m}$ ΔE and $2000\ \mu\text{m}$ E detector with appropriate tantalum collimators. Two Ge(Li) detectors were respectively placed at 90° and 55° with respect to the direction of recoil of the residual nuclei associated with protons detected in the telescope.

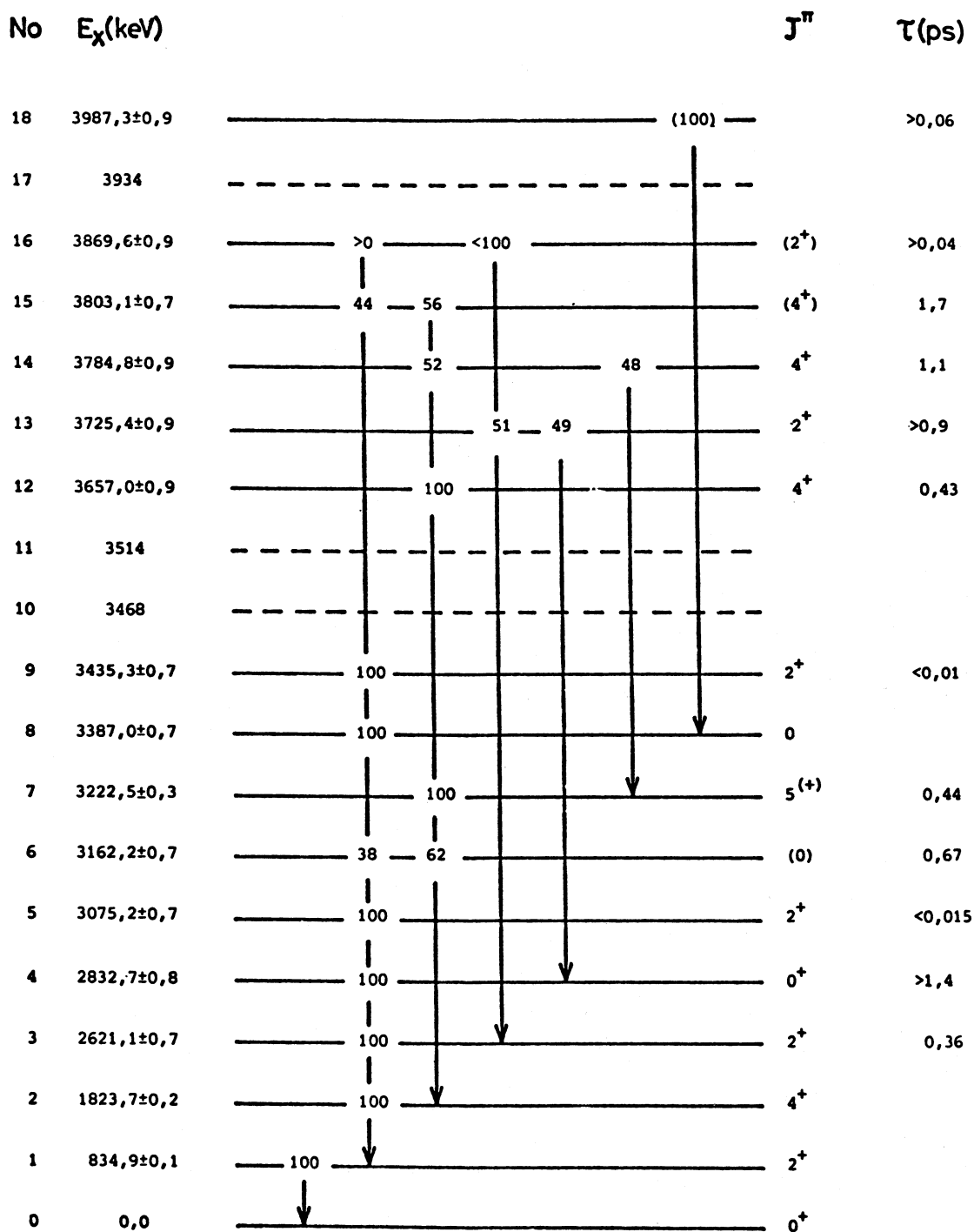
The target consisted of $135\ \mu\text{g}/\text{cm}^2$ natural vanadium on a $205\ \mu\text{g}/\text{cm}^2$ carbon backing and was placed at 90° to the beam direction. Data acquisition was effected by means of a 5-parameter coincidence system with ΔE , E , $\Delta E - E$ coincidence, gamma energy and E -gamma coincidence as the 5 parameters. In the off-line analysis of the data two more parameters, a particle identification spectrum and a $(\Delta E + E)$ energy spectrum were generated. The final results obtained from the analysis are shown in fig 1-18.

Information on the spins of levels in ^{54}Cr was obtained from a Hauser-Feshbach analysis of the relative behaviour of average cross sections of $^{51}\text{V}(\alpha, p\gamma)^{54}\text{Cr}$ reactions over an incident alpha energy range of 158 keV at $E_\alpha \sim 12\ \text{MeV}$. Protons were again detected by means of the telescope system in a 3-parameter arrangement employing particle identification. The telescope was placed at 120° with respect to the beam direction. Targets consisting of $75\ \mu\text{g}/\text{cm}^2$ and $115\ \mu\text{g}/\text{cm}^2$ V on $15\ \mu\text{g}/\text{cm}^2$ C were used and the beam energy was varied in 20 and 14 keV steps according to target thickness. Experimental cross sections deduced from the data were compared with theoretical predictions. Cross sections associated with levels with known spin were used for normalization. The most probable spin values obtained from the analysis are shown in fig 1-18.

1.2.4 Nuclear structure study of ^{37}Cl

- J J Laurie, W J Naudé

The energies, decay properties and lifetimes of states in ^{37}Cl were studied with $(p, p'\gamma)$, $(\alpha, \alpha'\gamma)$ and $(\alpha, p\gamma)$ reactions.

Fig. 1-18. Properties of energy levels in ^{54}Cr .

The $^{37}\text{Cl}(p,p'\gamma)^{37}\text{Cl}$ reactions were investigated at an incident proton energy of 6 MeV. Targets of BaCl_2 , enriched to 98 % in ^{37}Cl and prepared on carbon backings of $75 \mu\text{g}/\text{cm}^2$, were used in the measurements. By suitable coincidence registration using two proton detectors and one $\text{Ge}(\text{Li})$ detector, level energies, decay properties and lifetimes were determined simultaneously in a single experiment. Although analysis of the data is still in progress, results show that only levels up to about 4 MeV excitation are observed and that alternative reactions must be employed for the study of higher excitations.

To accomplish this, the $^{37}\text{Cl}(\alpha,\alpha'\gamma)^{37}\text{Cl}$ reactions were observed at $E_\alpha = 12$ MeV. The experimental arrangement was similar to that of the $(p,p'\gamma)$ study. For the lifetime measurements with the $(\alpha,\alpha'\gamma)$ reactions using Doppler-shift attenuation, BaCl_2 targets were carefully prepared on carbon backings of $500 \mu\text{g}/\text{cm}^2$ to ensure the complete deceleration of recoiling ^{37}Cl ions. The strong gamma ray yield from these carbon backings, necessitated the separation of level structure and decay measurements (using thin carbon backings) from lifetime measurements (with the thicker backings) and attention was initially given to the study of level energies and decay properties only.

A preliminary analysis of the results shows that excitation is selective in contrast with $(p,p'\gamma)$ reactions and that the mechanism is mainly Coulomb-excitation. It was thus decided to undertake yet another complementary study using $^{34}\text{S}(\alpha,p\gamma)^{37}\text{Cl}$ reactions at $E_\alpha = 12$ MeV. These reactions are weaker than (α,α') and (p,p') reactions but proceed mainly through the compound nucleus and are therefore non-selective as is the case for (p,p') reactions.

In the study of $^{34}\text{S}(\alpha,p\gamma)^{37}\text{Cl}$ reactions initial attention was given to the determination of level energies and decay properties. A target of $150 \mu\text{g}/\text{cm}^2$ Sb_2S_3 , enriched to 94 % in ^{34}S and prepared on a thin carbon backing, was used in the measurements. The experimental arrangement consisted of two $\text{Ge}(\text{Li})$ detectors and a ΔE -E telescope similar to the arrangement described in section 1.2.4. The ΔE counter used here was a $18 \mu\text{m}$ surface barrier transmission detector.

2. PHYSICS DIVISION, ATOMIC ENERGY BOARD, PELINDABA, TRANSVAAL

The research program relevant to this report is based on the research reactor, Safari I and the 3,75 MV pulsed Van de Graaff accelerator.

2.1 Thermal-neutron capture

- C Hofmeyr and C B Franklyn

Measurements have been made of coincident gamma rays from the de-excitation of ^{86}Rb produced by thermal neutron capture in ^{85}Rb , using $\text{Ge}(\text{Li})$ detectors.

The coincidence spectra are being analysed using the peak fitting routine SAMPO. The results should resolve the anomaly in the intensity balance between the high energy and low energy level transitions, which in present literature contains discrepancies of up to a factor of 3.

2.2 Neutron angular correlations in fission

- C B Franklyn and C Hofmeyr

A simple evaporation model of fission, taking into account kinematical factors, has shown that detailed measurements of the prompt-neutron fission-fragment angular correlation at small angles to the fission axis are necessary to determine the magnitude of the scission-neutron emission anisotropy. A new fission chamber detection system is now being tested prior to measuring the fission neutron-fragment angular correlation for ^{252}Cf spontaneous fission and thermal neutron induced fission in ^{235}U . The results so obtained will complement previous measurements of the fission neutron-neutron angular correlations.

2.3 Inelastic scattering of fast neutrons

- E Barnard, D W Mingay and D Reitmann

The level schemes of ^{85}Rb and ^{87}Rb have been investigated by means of the $(n,n'\gamma)$ reaction at neutron energies between 800 and 2100 keV using a natural Rb sample. Six new energy levels in ^{85}Rb have been identified, all other level energies have been determined more precisely and several inconsistencies in the decay scheme have been resolved. In ^{87}Rb , evidence shows that the level at 1349.6 keV, previously derived from beta decay results, should be removed from the level diagram. At least two previously unknown gamma transitions and one new energy level are observed.

Branching ratios and gamma-ray production cross sections were determined and, in the latter case, compared with experimental results from neutron time-of-flight experiments as well as with calculations employing the optical model and Hauser-Feshbach theory. This led to the assignment of spins and parities to a number of levels. The final results for Rb are shown in fig 2-1, where asterisks indicate previously unknown transitions and energy levels.

A series of (n,n') measurements were performed on a natural Ag sample in order to compare the absolute scattering cross sections thus obtained with the previous $(n,n'\gamma)$ results for Ag, which are still being processed.

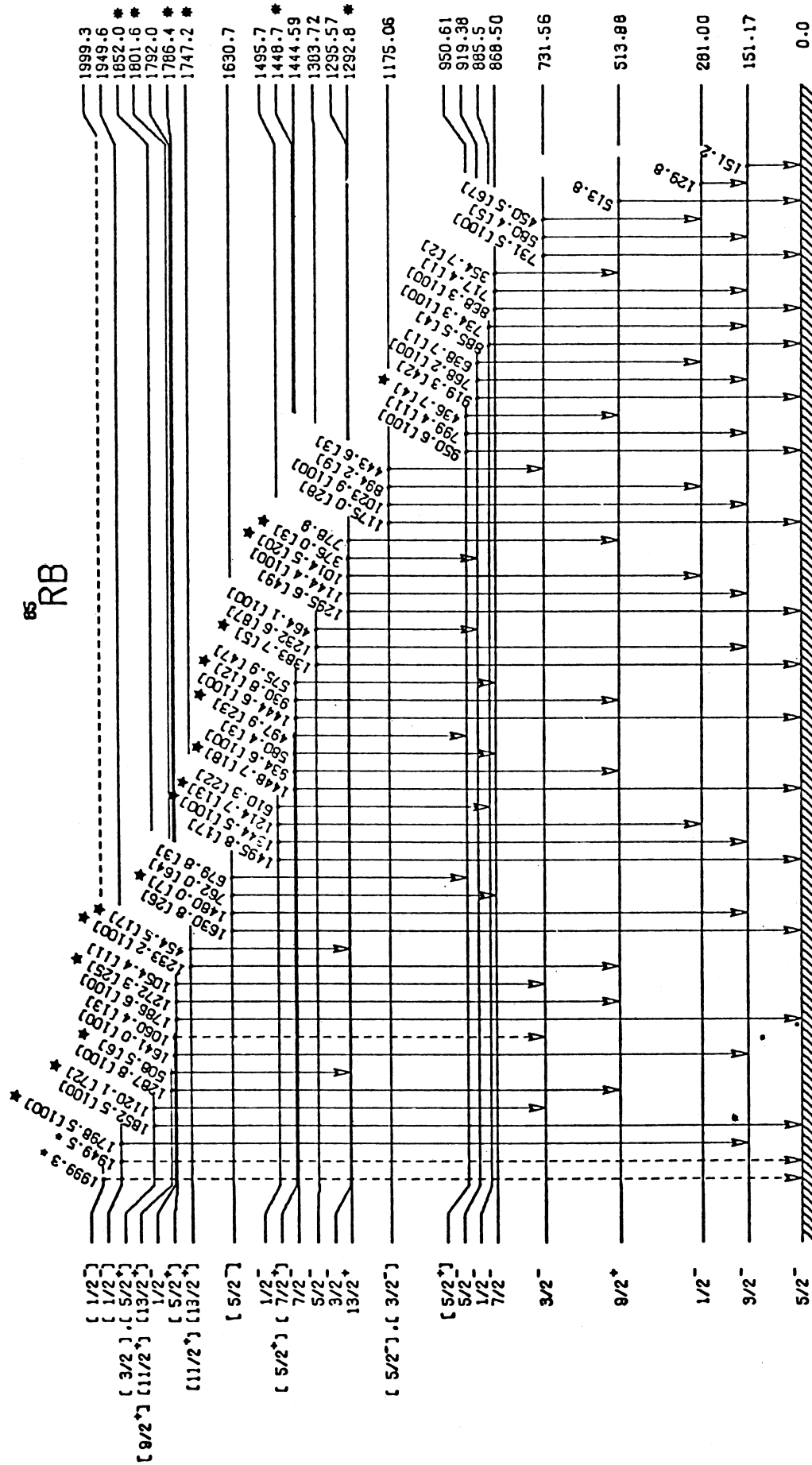


Fig 2-1

Data from a series of $(n,n'\gamma)$ measurements on Au are still being analysed. Because of the complexity of the level scheme and the large number of gamma rays which have to be fitted into a level diagram, additional measurements with good energy resolution and calibration were done at an incident neutron energy of 2.1 MeV. A large number of previously unknown energy levels in ^{197}Au are indicated by the results.